Geol. Mag. **156** (2), 2019, pp. 281–307 © Cambridge University Press 2018
doi:10.1017/S0016756818000031

The pre-orogenic detrital zircon record of the Peri-Gondwanan crust

TOBIAS STEPHAN*†, UWE KRONER* & ROLF L. ROMER‡

*Institut für Geologie, TU Bergakademie Freiberg, B. v. Cotta Str. 2, 09599 Freiberg, Germany
‡Deutsches GeoForschungsZentrum GFZ, Telegrafenberg, 14473 Potsdam, Germany

(*Received* 3 July 2017; *accepted* 29 December 2017; *first published online* 8 February 2018)

Abstract – We present a statistical approach to data mining and quantitatively evaluating detrital age spectra for sedimentary provenance analyses and palaeogeographic reconstructions. Multidimensional scaling coupled with density-based clustering allows the objective identification of provenance end-member populations and sedimentary mixing processes for a composite crust. We compiled 58 601 detrital zircon U–Pb ages from 770 Precambrian to Lower Palaeozoic shelf sedimentary rocks from 160 publications and applied statistical provenance analysis for the Peri-Gondwanan crust north of Africa and the adjacent areas. We have filtered the dataset to reduce the age spectra to the provenance signal, and compared the signal with age patterns of potential source regions. In terms of provenance, our results reveal three distinct areas, namely the Avalonian, West African and East African–Arabian zircon provinces. Except for the Rheic Ocean separating the Avalonian Zircon Province from Gondwana, the statistical analysis provides no evidence for the existence of additional oceanic lithosphere. This implies a vast and contiguous Peri-Gondwanan shelf south of the Rheic Ocean that is supplied by two contrasting super-fan systems, reflected in the zircon provinces of West Africa and East Africa–Arabia.

Keywords: palaeogeography, Gondwana, zircon provenance, U–Pb dating, multidimensional scaling, clustering, Variscides

1. Introduction

Palaeogeographic information provides key starting constraints for plate tectonic reconstructions, in particular for the provenance of terranes and microcontinents that become amalgamated to larger continental masses during collisional processes. The most widely used palaeogeographic indicators include palaeoclimatologic, palaeobiographic and palaeomagnetic data and provenance analysis of detrital heavy minerals (e.g. Van der Voo, 1988; McLennan *et al.* 1993; Morton & Hallsworth, 1994; Torsvik *et al.* 1996; Scotese, Boucot & McKerrow, 1999; Golonka & Ford, 2000; Cocks & Torsvik, 2002; Fedo, Sircombe & Rainbird, 2003). Geochemical and isotope-geochemical fingerprints generally do not provide unambiguous constraints (Arndt & Goldstein, 1987). Furthermore, palaeomagnetic data lack spatial resolution as the latitudinal position of individual tectonic blocks may have an uncertainty range of as large as 40° (in the case of the Early Palaeozoic Peri-Gondwanan shelf, see fig. 11 in Franke, Cocks & Torsvik, 2017 and references therein).

The possibility to date detrital heavy minerals and, therefore, to constrain the age of the igneous and/or high-grade metamorphic protoliths of sedimentary rocks has gained tremendous significance since the early studies by Ledent, Patterson & Tilton (1964) and Tatsumoto & Patterson (1964). In particular, the development of the high spatial resolution analytical tools of secondary ion mass spectrometry (SIMS) and laser ablation inductively coupled plasma mass spectrometry (LA-ICP-MS) has made U–Pb dating of detrital minerals, particularly zircon, the most applied approach in provenance analyses. In comparison to other methods, SIMS and LA-ICP-MS U–Pb dating of zircons provides, with relative ease, palaeogeographic constraints in the form of age spectra that fingerprint the source or sources of detrital zircons in sedimentary rocks. Since its first applications, U–Pb dating of detrital minerals has produced the largest database of provenance.

The subjective comparison of individual zircon age spectra with each other or with likely source areas is in many cases inadequate, as the pattern may be changed during erosion of the source and transport to the sink and, therefore, the similarity of pattern alone is not always conclusive (e.g. Blatt, 1967; Dickinson & Gehrels, 2009*a*; Hietpas *et al.* 2011; Zimmermann *et al.* 2015). For instance, high-topography (generally young) areas are subject to stronger erosion than deeply eroded low-topography (old or stable) areas and, therefore, zircons derived from the high-topography areas are likely to be overrepresented in the zircon age spectra. Especially in datasets that are dominated by zircons from the youngest magmatic or metamorphic event, the age distribution of older inherited zircons may not be representative (Cawood,

†Author for correspondence: tobias.stephan@geo.tu-freiberg.de

Hawkesworth & Dhuime, 2012, 2013). Similarly, multiple recycling and redeposition of sediments and sedimentary rocks may change the age spectra or result in mixed age spectra with material from different sources (e.g. Blatt, 1967; Moecher & Samson, 2006; Dickinson & Gehrels, 2009*a*; Hietpas *et al.* 2011; Hawkesworth, Cawood & Dhuime, 2013; Zimmermann *et al.* 2015; Andersen, Kristoffersen & Elburg, 2016). Some of these problems may be reduced or avoided by using large, compiled datasets and applying quantitative filtering and data evaluation techniques. Statistical data analysis has become possible because of the increasing number of high-quality datasets on the age distribution of detrital zircons.

We present a simple yet powerful approach to statistical data mining and quantitatively evaluating detrital age spectra that allows the identification of provenance end-member populations for a composite crust. We tested the zircon provenance analysis for the Peri-Gondwanan crust north of Africa and adjacent areas for the following reasons: (i) a huge dataset is available for statistical treatment; (ii) there exists detailed geological background information; and (iii) there exists a wide range of tectonic fragments of potentially contrasting provenance that have been juxtaposed during the Variscan orogeny. We compiled 58 601 U–Pb ages from 770 Precambrian to Lower Palaeozoic sedimentary rocks from 160 publications, filtered the dataset to reduce the age spectra to the provenance signal, and compared the provenance signal with age patterns of potential source regions. The resulting provenance map for the Variscan orogen provides fundamental constraints against which published tectonic models, suggested litho-biostratigraphic correlations among different terranes, and the palaeogeographic reconstruction of Peri-Gondwana are tested and in part disqualified.

2. Tectonic elements of the Peri-Gondwanan shelf

2.a. The assemblage of Pangaea

The assembly of the Phanerozoic supercontinent Pangaea encompasses the Palaeozoic convergence of the Gondwana and Laurussia plates. It culminated in the Caledonian and Variscan orogenies by affecting the northern Lower Palaeozoic continental shelf of the Gondwana plate, i.e. Peri-Gondwana, which was situated north of the Amazonas Craton, the West African Craton, the Sahara Metacraton and the Arabian–Nubian Shield. The shelf comprises blocks of Neoproterozoic–Cambrian basement overlain by Lower Palaeozoic volcano-sedimentary successions (e.g. Robardet *et al.* 1994; Gutiérrez-Marco *et al.* 2002; Linan *et al.* 2002; Geyer *et al.* 2008; Servais *et al.* 2008).

The different initial position along the shelf and the contrasting pre-Variscan tectonic history resulted in three provinces of distinctive fauna (e.g. Robardet *et al.* 1994; Scotese, Boucot & McKerrow, 1999; Cocks & Torsvik, 2002), isotopic signature (Henderson *et al.* 2016) and detrital heavy mineral composition of the sedimentary cover of the Peri-Gondwanan crust (e.g. Fernández Suárez *et al.* 1998; Friedl *et al.* 2000; Bea *et al.* 2010; Dörr *et al.* 2015; Henderson *et al.* 2016): (i) Avalonia (north of the Rheic suture), (ii) West Africa and (iii) East Africa–Arabia. Cambro-Ordovician rifting along the Cadomian–Avalonian belt led to the opening of the Rheic Ocean, thereby separating Avalonia from mainland Gondwana (e.g. Paris & Robardet, 1990; Veevers, 2004; Nance & Linnemann, 2008; Nance *et al.* 2010). Coeval to seafloor spreading, intracontinental extension resulted in the formation of extended Peri-Gondwanan shelf areas north and south of the intervening Rheic Ocean (e.g. Cocks, McKerrow & Van Staal, 1997; Van Staal *et al.* 1998; Kroner & Romer, 2013; Stampfli *et al.* 2013). After the Caledonian collision of Avalonia with the East European Craton and Laurentia to form Laurussia during the Late Ordovician–Silurian period (Torsvik & Rehnström, 2003), the southern boundary of Avalonia developed into an active margin resulting in the subduction of the Rheic Ocean (Nance *et al.* 2010 and references therein). Diachronous collision of Peri-Gondwanan crust with Laurussia caused the Early Devonian–Permian Acadian–Variscan–Alleghenian orogeny (e.g. Matte, 2001; Kroner & Romer, 2013; Stampfli *et al.* 2013; Franke, Cocks & Torsvik, 2017), thereby forming Western Pangaea, and eventually resulted in syn-collisional escape and strike-slip tectonics (e.g. Arthaud & Matte, 1977; Martínez Catalán, 2012; Kroner, Roscher & Romer, 2016; Stephan *et al.* 2016). Owing to the complex history of the opening and closure of the Rheic Ocean with shelf fragmentation and displacement during collision, respectively, the provenance of individual blocks may be ambiguous. For example, the Ibero-Armorican Arc shows provenance features that have typically been ascribed to Avalonia (e.g. Braid *et al.* 2011; Pérez-Cáceres *et al.* 2017) and West Africa (e.g. Linnemann *et al.* 2008*b*; Díez Fernández *et al.* 2010; Strachan *et al.* 2014) as well as East Africa–Arabia (e.g. Shaw *et al.* 2014; Orejana *et al.* 2015). Moreover, as evidenced in the Mediterranean, post-Pangaea divergent and convergent tectonics of micro-continental blocks (e.g. Schmid *et al.* 2004; Handy, Ustaszewski & Kissling, 2015) further enhance the complexity of the Peri-Gondwana provenance pattern.

2.a.1. *Avalonia*

As part of Peri-Gondwana, Avalonia contains remnants of the Cadomian magmatic arc that are only exposed in a few small tectonic inliers of East Avalonia, i.e. in the Midland Craton, northern and southern Wales, and Ireland, as well as in Silesia and Małopolska (O'Brien, Wardle & King, 1983; Dudek, 1995; Molzahn, Anthes & Reischmann, 1998; Breitkreuz & Kennedy, 1999; Pharaoh, 1999; Belka *et al.* 2000; Verniers *et al.* 2002; Krawczyk *et al.* 2008). The rocks are dominated by

700–540 Ma old volcano-sedimentary successions that have been intruded by *c*. 620–540 Ma old I-type granitoids (Pharaoh & Carney, 2000; Linnemann *et al.* 2008*b*; Moryc & Łydka, 2012; Strachan, 2012).

Upper Proterozoic to Ordovician siliciclastic rocks are characterized by thick turbiditic sequences, which were in part deposited in graben systems that developed during the rifting of Peri-Gondwana. The decoupling of Avalonia from Gondwana is recorded in the change from Early Ordovician Gondwanan faunal signatures to Silurian faunas of Laurentian affinity, i.e. the transition from a cool-water, high-latitude environment (Gondwana) to warmer, lower latitude conditions, i.e. Laurentia (Boyce, Ash & O'Brien, 1991; Williams, 1993; Dean *et al.* 2000; Chen *et al.* 2002; Oczlon, Seghedi & Carrigan, 2007; Pollock, Hibbard & van Staal, 2011). The separation of Gondwana is accompanied by Middle Cambrian to Early Ordovician bimodal volcanism in Avalonia (White *et al.* 1994; Johnson & McLeod, 1996; Rogers *et al.* 2006; Schulz *et al.* 2008; Dunning *et al.* 2009).

The docking of Avalonian terranes to Laurentia is underlined by Early to Middle Ordovician obduction of ophiolites on both Laurentia and Avalonia (Zagorevski *et al.* 2010). The Early Ordovician rifting from Gondwana and the Late Ordovician docking of East Avalonia to Laurentia (Torsvik & Rehnström, 2003) are coeval to those in the Meguma and West Avalonian terranes (Keppie & Krogh, 2000; MacDonald *et al.* 2002).

Post-rifting overstep sequences are characterized by Ordovician manganese-rich sedimentary rocks (Kramm, 1976; Jimenez Millan & Velilla, 1998; Kennan & Morris, 1999; Dill *et al.* 2008). Because these lithologies are not known from Peri-Gondwanan domains south of the Rheic Ocean, this exclusive feature may serve as a palaeogeographic proxy (Romer, Kirsch & Kroner, 2011). From the Late Ordovician epoch onwards, Avalonia received detritus from the erosion of the Caledonides due to the connection with Baltica (Belka & Narkiewicz, 2008; Verniers *et al.* 2008).

2.a.2. *Northern Gondwana*

The basement of the West African and the East African–Arabian part of Peri-Gondwana consists of the Cadomian magmatic arc combined with volcano-sedimentary rocks that have been intruded by voluminous I-type granitoid bodies of regionally different ages between 620 and 530 Ma (J. J. Beetsma, unpub. Ph.D. thesis, Vrije Universiteit Amsterdam, 1995; Linnemann *et al.* 2000, 2008*a*,*b*, 2010*b*; Ballèvre, Le Goff & Hébert, 2001; Chantraine *et al.* 2001; Pereira *et al.* 2006; Ezzouhairi *et al.* 2008; Talavera *et al.* 2012).

The overlying Upper Proterozoic to Cambrian sedimentary sequences are characterized by siliciclastic erosional debris from the former Cadomian (e.g. Linnemann *et al.* 2014; Žák & Sláma, 2017) and Pan-African magmatic arcs (e.g. Balintoni *et al.* 2009; Pereira, 2015) and from the recycled Gondwanan continental crust (e.g. Meinhold, Morton & Avigad, 2013; Rösel *et al.* 2014). The Upper Cambrian to Ordovician sedimentary deposits are dominated by highly mature rocks that may reach several thousand metres thickness. These sediments originally experienced intense chemical weathering on a stable continent and were redistributed to the continent margin during the early stages of the rifting of the Rheic Ocean with decreasing detritus from the Cadomian arc (Pique & Michard, 1989; Nägler, Schafer & Gebauer, 1995; J. J. Beetsma, unpub. Ph.D. thesis, Vrije Universiteit Amsterdam, 1995; Linnemann *et al.* 2000, 2010*a*; Avigad *et al.* 2005; Romer & Hahne, 2010).

A local tectonic feature of the Peri-Gondwanan crust is the so called 'Sardic phase' that is recorded as a 457–443 Ma tectono-metamorphic event in Middle Ordovician rocks of the Agordo basement and the Strona–Ceneri Zone of the Southern Alps and in parts of the Carpathians (Poli & Zanferrari, 1992; Franz & Romer, 2007; Zurbriggen, 2015) and as a pronounced unconformity in the shelf sediments of the Montagne Noire, the Mouthoumet Massif, the Eastern Pyrenees, the Catalonian Coastal Ranges, the Central Iberian Zone, Sardinia, Corsica, Sicily and in southern Turkey (Lotze, 1956; Carmignani *et al.* 1982; Gil Ibarguchi, Navidad & Ortega, 1990; Gutiérrez-Marco, De San José & Pieren, 1990; Hammann, 1992; Robardet *et al.* 1994; Valverde-Vaquero & Dunning, 2000; Trombetta *et al.* 2004; Rossi, Oggiano & Cocherie, 2009; Javier Álvaro *et al.* 2016; Cocco & Funedda, 2017). According to Gutiérrez-Marco *et al.* (2002 and references therein), echoes of the Sardic event may be represented by oolitic iron beds in Iberia. It is worth noting that the Sardic event is unknown in the Ossa-Morena Zone, the Armorican Massif, the Bohemian Massif and adjacent areas.

The Upper Ordovician sequences of northern Gondwana are dominated by the widespread occurrence of glaciomarine tillites that are indicative of the glaciation of northern Gondwana (Ghienne, 2003 and references therein). However, contemporaneous tillites are not known from Avalonia, which must have drifted away from Gondwana earlier. Thus, the glaciomarine tillite represents a tracer to assign individual crustal fragments to the southern passive margin of the Rheic Ocean, i.e. to Gondwana during the Late Ordovician epoch (Linnemann & Heuse, 2000).

2.b. Tectonic models for the pre-Pangaea stage

There is broad consensus about the plate tectonic kinematics of Avalonia, which separated from Gondwana at *c*. 480 Ma (Cocks & Fortey, 1982) and collided with the East European Craton (Baltica) in the Late Ordovician epoch (Torsvik & Rehnström, 2003). However, apart from explanations of tectono-metamorphic processes during the formation of Western Pangaea culminating in the Variscan orogeny, there are

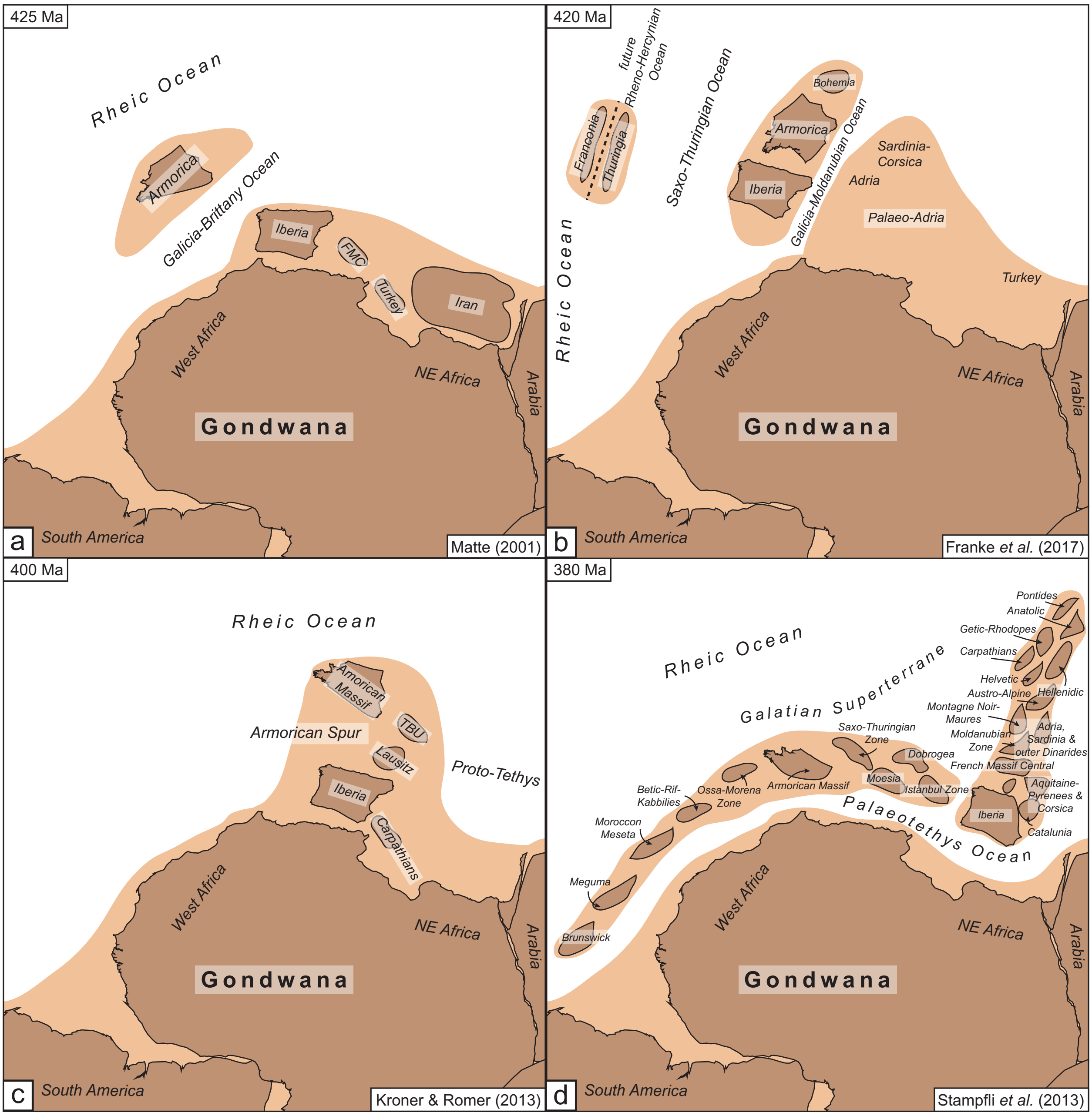

Figure 1. (Colour online) Tectonic models of pre-Pangaean palaeogeography and architecture of Peri-Gondwana. Note the different number of involved plates and oceans and the position of Iberia. Modified after Matte (2001), Franke, Cocks & Torsvik (2017), Kroner & Romer (2013) and Stampfli *et al.* (2013). Orthographic projection.

several tectonic models that rely on contrasting starting conditions, including a different number of involved plates and oceans and different initial positions along the Peri-Gondwanan shelf south of the Rheic Ocean (Fig. 1):

(i) Matte (1986) explained the distribution of subduction-related high-pressure domains within the Variscan belt by closure of two oceanic domains (Rheic Ocean in the north, and Galicia–Brittany Ocean in the south) involving the collision of three lithospheric plates (Gondwana, Armorica and Laurussia) with initial subduction beneath the intervening Armorican microplate. Prior to the opening of the Galicia–Brittany Ocean, the Armorican microplate as well as the Peri-Gondwanan fragments were attached adjacent to the West African Craton with Iberia in the westernmost position.

(ii) Palaeomagnetic studies (Tait *et al.* 1997) challenged this model by suggesting that Peri-Gondwana represents an assemblage of microplates that have been separated by individual oceans during the Ordovician–Early Devonian epoch and have been juxtaposed during the Variscan orogeny (Franke, 2000; Torsvik & Cocks, 2013; Franke, Cocks & Torsvik, 2017). Similar to Matte (1986), all microplates were initially located adjacent to the West African Craton.

(iii) Because of striking similarities between sedimentological and faunal data (e.g. Young, 1990;

Robardet, 2002), the same geochemical fingerprint of deep chemical weathering (e.g. Noblet & Lefort, 1990; Romer & Hahne, 2010; Ugidos *et al.* 2010), and geochronological, isotope-geochemical data and provenance data (e.g. Linnemann *et al.* 2004) of Cambrian to Devonian sedimentary rocks covering the basement of the Armorican Terranes, Kroner *et al.* (2007) proposed that Peri-Gondwana south of the Rheic Ocean represents an extended shelf of the Gondwana plate comprising Cadomian blocks that are separated by thinned continental crust. Kroner & Romer (2010) introduced the term 'Armorican Spur' and explained the Variscan orogeny as the exclusive result of the collision between the two plates of Gondwana and Laurussia subsequent to the closure of the Rheic Ocean. Iberia is placed in a central position of the spur. Coeval to the ongoing Gondwana–Laurussia convergence, the Devonian opening of the Palaeotethys Ocean occurred east of the Armorican Spur (Kroner & Romer, 2010, 2013) due to plate tectonic reorganization processes (Kroner, Roscher & Romer 2016).

(iv) Alternatively, Stampfli & Borel (2002) placed all Peri-Gondwanan fragments together with Asian terranes such as Turkey, Turan (Iran), Pamirs, Tarim and North China in a coherent ribbon-like terrane, i.e. the so called 'Hun Superterrane', that detached from Gondwana during the opening of the Palaeotethys Ocean during the Late Ordovician–Silurian period. The assembly is mainly based on the distribution of Cambrian–Devonian carbonate platforms and the Cambro-Ordovician drifting patterns. Later, Stampfli *et al.* (2013) rejected the model of a coherent Hun Superterrane. The newly defined 'Galatian Superterrane' contains the entire Peri-Gondwanan crust south of the Rheic Ocean and north of Africa (Fig. 1) and remained an integral part of Gondwana until the Devonian period. Owing to the Devonian opening of the Palaeotethys Ocean, this ribbon continent rifted off from Gondwana and collided with Laurussia not before the Late Visean final stage of the Variscan orogeny.

3. Methods

3.a. Database selection and pre-processing

Age spectra of Precambrian to Lower Palaeozoic samples were constructed on the basis of detrital zircon U–Pb ages from 160 publications (Fig. 2). The compilation combines single grain age data obtained by thermal ionization mass spectrometry (TIMS), LA-ICP-MS and SIMS (Tables S1, S2 in the online Supplementary Material available at http://journals.cambridge.org/geo). To uncover provenance patterns of the age spectra of each sample, we filtered the dataset as follows:

(i) We exclusively used samples that were deposited before 400 Ma, i.e. pre-Variscan samples (if the sample age was not given by the authors, we have used the age of the youngest zircon population as the minimum estimate for the deposition age) (Dickinson & Gehrels, 2009*b*).

(ii) The entire dataset was re-processed using a common age calculation and concordance filter to ensure comparability (Table S3 in the online Supplementary Material available at http://journals.cambridge.org/geo). To guarantee that only concordant grains, i.e. with <10 % normal and <5 % reverse discordance, were included in the age compilation, the concordance of zircon grains older than 1000 Ma were calculated from their ^{206}Pb–^{238}U and ^{207}Pb–^{206}Pb ages and those of zircon grains younger than 1000 Ma were calculated from their ^{206}Pb–^{238}U and ^{207}Pb–^{235}U ages. Note, using ^{207}Pb–^{206}Pb ages to estimate discordance of Phanerozoic zircons may result in apparent discordance as for geologically young samples the intersection between the discordia reflecting the ^{207}Pb–^{206}Pb age and the concordia has a very flat angle. Even a small error in the $^{207}Pb/^{206}Pb$ ratio has a major effect on the apparent ^{207}Pb–^{206}Pb age (e.g. Mattinson, 1987). Because of the shape of the concordia, which flattens for older ages, the intersection of the $^{207}Pb/^{206}Pb$ discordia and the concordia is better defined for older ages. For the data analysis, we used, therefore, the ^{206}Pb–^{238}U age for Phanerozoic and Neoproterozoic zircons and the ^{207}Pb–^{206}Pb age for zircons older than 1000 Ma.

(iii) Statistical data analysis, especially multidimensional scaling, is strongly influenced by large populations. The majority of the pre-Variscan samples, however, are affected by the Variscan and Cadomian orogeny, which eventually results in the overrepresentation of younger zircon grains. Statistical analysis of the entire age spectrum of each sample will put a much higher weight on these late events, which are of little relevance for provenance analysis, and only a little weight on the older zircon populations. Statistical data treatment may yield a different result if only the relevant portion of the spectrum is included in the dataset. For provenance analysis, the relevant information is preserved in the older detrital record (Cawood, Hawkesworth & Dhuime, 2013). Therefore, all zircon age spectra have been truncated to include exclusively pre-Cadomian ages, i.e. >700 Ma.

(iv) For detrital zircon data, the statistical adequacy, i.e. the extent to which the observed age abundance matches the corresponding abundance in the sediment, is influenced by the number of grains analysed (Vermeesch, 2004; Andersen, 2005; Pullen *et al.* 2014) and by the sample preparation procedure (Sláma & Košler, 2012). An insufficient number of zircon grains analysed per sample, i.e. $k < 117$, may cause certain age populations to go undetected or result in spurious peaks in the age spectra (Sircombe, 2000; Vermeesch, 2004). The premise of a minimum of $k = 117$ ages (Vermeesch, 2004) refers to the original dataset, but is unwarranted after the exclusion of parts of the age spectrum. Cadomian ages amount to more than 75 % of the total age spectra in the majority of the compiled samples. For instance, a notional sample comprising 117 ages satisfies the condition, but it

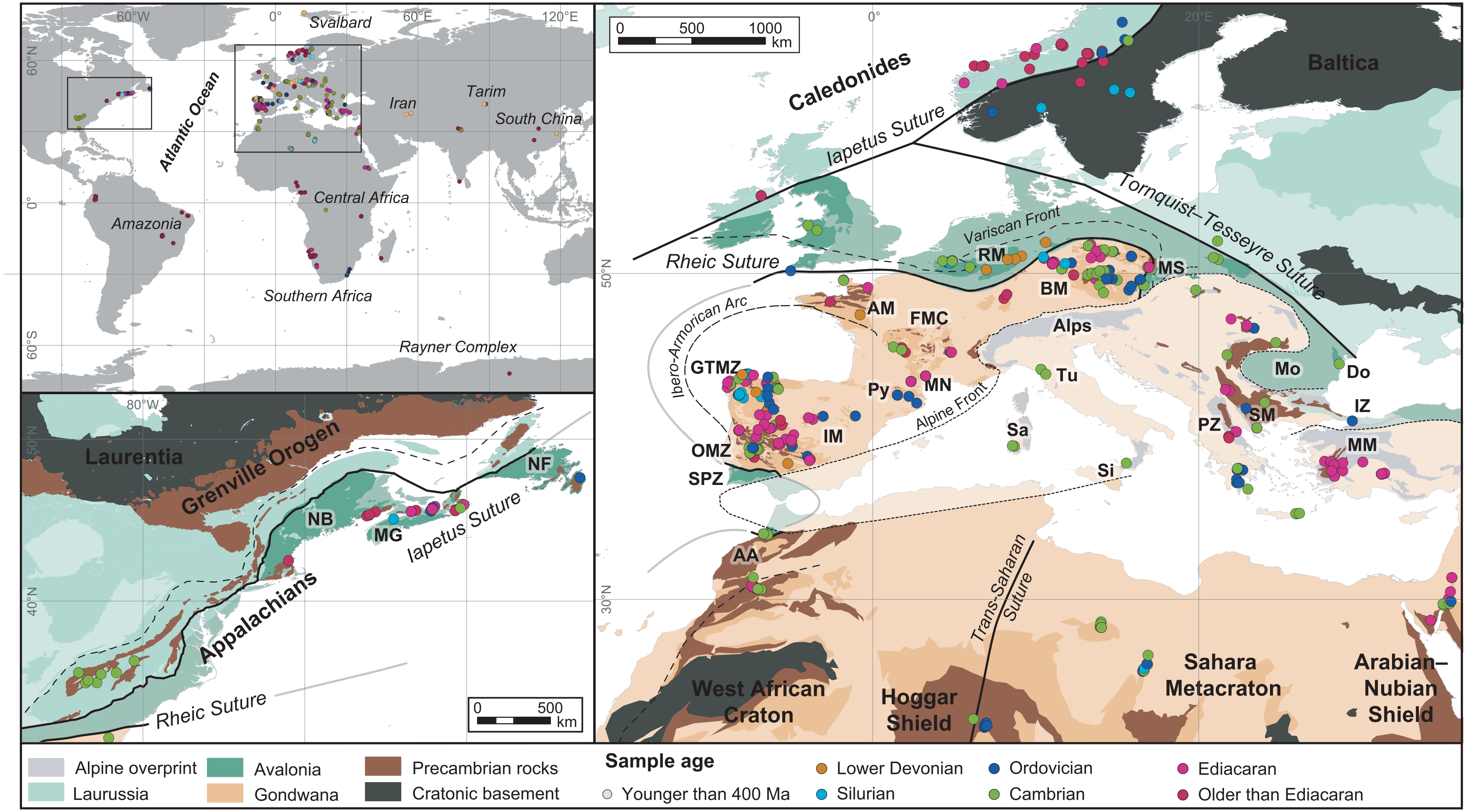

Figure 2. (Colour online) Simplified tectonic map with location of the investigated samples. Abbreviations: AA – Anti-Atlas; AM – Armorican Massif; BM – Bohemian Massif; Do – Dobrogea; GTMZ – Galicia–Trás-os-Montes Zone; FMC – French Massif Central; IM – Iberian Massif; IZ – Istanbul Zone; MG – Meguma; MM – Menderes Massif; Mo – Moesia; MS – Moravo-Silesian Zone; NB – New Brunswick; NF – Newfoundland; OMZ – Ossa-Morena Zone; Py – Pyrenees; PZ – Pelagonian Zone; RM – Rhenish Massif; Sa – Sardinia; Si – Sicily; SM – Serbo-Macedonian Massif; SPZ – South Portuguese Zone; Tu – Tuscany. A georeferenced kmz file (S4) of the sample locations is provided in the online Supplementary Material available at http://journals.cambridge.org/geo.

contains 88 Cadomian ages and 29 ages of the proper provenance. In order to preserve the proportional fraction in a statistically minimal input, we solely included samples containing more than 30 concordant ages in the >700 Ma age compilation.

3.b. Multidimensional scaling

Provenance analysis that is based on geochronological data requires comparison of the age distributions between the samples. Our dataset comprising $n = 705$ age distributions would result in $n(n-1)/2 = 248\,160$ pairwise comparisons, which is definitely not feasible to do visually.

Mathematically, the similarity between two objects can be expressed as the distance between these objects within Euclidean space. Because the geochronological space is a functional space, it has to be transformed into Euclidean space. Multidimensional scaling (MDS) is a dimension-reducing algorithm that transfers the Kolmogorov–Smirnov dissimilarities between samples into Euclidean distances between the corresponding points within a multidimensional space (Vermeesch, 2013).

An advantage of MDS is the sample-size independence of the Kolmogorov–Smirnov test for a population size larger than 30 (Geweke & Singleton, 1980; Bearden, Sharma & Teel, 1982; Razali & Wah, 2011). The technique has been successfully applied in several provenance studies (Stevens *et al.* 2013; Nie *et al.* 2014; Arboit *et al.* 2016; Rittner *et al.* 2016).

The resulting output matrix (MDS configuration) gives the (dis)similarity among the various data as coordinates in a geometric space. The dimensionality is chosen by the user. The more dimensions, the better the statistical fit of the data and the lower the significance of the various dimensions. We applied a three-dimensional solution to describe the variation of the large sample set.

3.c. Clustering the dataset

To objectively identify groups of similar age signature, i.e. provenance, we clustered the MDS data by using the corresponding Kolmogorov–Smirnov dissimilarities. The choice of the clustering algorithm depends on the MDS configuration. On the one hand, there is little domain knowledge to determine the input parameters in advance, e.g. the number of clusters and the presence of outliers. On the other hand, the algorithm has to discover clusters with arbitrary shapes, because the shapes of clusters in three-dimensional MDS may be, for instance, spherical, drawn-out, linear or elongated. We applied two cluster algorithms for the following reasons:

(i) Small sample size leads to a noisy MDS configuration as age populations may remain undetected. Classic clustering algorithms, e.g. k-means or hierarchical methods, are unable to discriminate between outliers and proper groups of data (Ester *et al.* 1996). The source fingerprint of a sample may be blurred if recycling processes and/or sediment mixing took place during source-to-sink transport. Simple two-component mixing of two end-members results in elongate MDS configurations, whereas contributions from several sources or several processes result in irregular MDS configurations. The shape may be more arbitrary if several sources or processes are involved. The number of potential sources within the dataset, which is necessary information to determine the number of clusters, is unknown and, therefore, has to be estimated indirectly from the density of the data. For instance, Density-Based Spatial Clustering of Application with Noise (DBSCAN) is an algorithm aimed to detect outliers and handle arbitrary cluster shapes (Ester *et al.* 1996). The principle is that for each point of a cluster the neighbourhood of a given radius has to contain at least a minimum number of points, i.e. the density in the neighbourhood of the point has to exceed some threshold. Hierarchical Density-Based Spatial Clustering of Application with Noise (HDBSCAN) computes the hierarchy of all DBSCAN clusterings, and then uses a stability-based extraction method to find optimal cuts in the hierarchy by defining the minimum number of points within a cluster as the only input parameter (Campello, Moulavi & Sander, 2013).

(ii) MDS configurations with little or no noise are suitable for discrimination by hierarchical clustering analysis. This algorithm builds the hierarchy from the individual samples by progressively merging similar clusters. The similarity is expressed in pairwise Euclidean distances and the agglomeration results are presented in a dendrogram. The agglomeration is stopped when a sufficiently small number of clusters is achieved or the distances between cluster agglomerations exceeds a certain threshold. Both the number of clusters and the distances between cluster agglomerations, which are the input parameters for the clustering, are unknown and have to be estimated by the user. To avoid subjective interference in the cluster result, the unsupervised learning algorithm 'gap statistic' can estimate the optimal number of clusters (Tibshirani, Walther & Hastie, 2001). The method uses the output of clustering and compares intra-cluster scattering with the scatter expected under a null reference distribution of the data, i.e. a distribution with no obvious clustering. Varying the number of clusters as the input parameter, the optimal number of clusters corresponds to the set up that yields the largest gap between both intra-cluster scatterings. The clustering result is validated and, if necessary, optimized by using a silhouette plot. The silhouette method tests for consistency within clusters by comparing the similarity of a sample i to its own cluster and to the other clusters (Rousseeuw, 1987). The silhouette width generally ranges from –1 to 1. A value close to 1 indicates that the sample lies within its own cluster. If a sample lies between its assigned cluster and another one, the silhouette is between 0 and 1. Low or negative values mean the sample lies within another cluster indicating poor clustering or assignment to the wrong cluster. The next best fit cluster corresponds to the 'neighbour' that represents the cluster with the lowest average dissimilarity to a particular sample. The quality of the clustering is measured by the average silhouette over all the data of the entire dataset.

3.d. Reading cluster-coupled multidimensional scaling

Classic detrital zircon provenance analysis compares the zircon age spectra of sedimentary rocks from a sink area with the age spectra of magmatic (and metamorphic) events of different cratonic source areas. The source with the highest similarity to the sink is interpreted to be the provenance. Thus, an MDS cluster containing a compilation of magmatic and metamorphic events of a potential source represents a group of sedimentary rocks with mutual provenance. However, the shape of an MDS configuration depends on the number of sources (or provenances) and the sedimentary recycling and mixing processes involved during the source-to-sink transport. A simple two-provenance mixing results in an elongate MDS configuration with each provenance at the respective ends of the elongated MDS shape ('end-member'). The 'mixing line' between the end-members indicates sedimentary mixing or recycling of both provenances (Vermeesch, 2013; Sharman & Johnstone, 2017).

The underlying premise of this approach is a complete knowledge of the history of the source, as statistical data analysis of incomplete age spectra may result in meaningless or spurious outputs (see discussion in Section 3.a). The geochronological database of magmatic-metamorphic events of the Precambrian basement of northern Africa (e.g. Sahara Metacraton) is likely to be incomplete, as the craton is poorly exposed and northern Africa was an area of sediment accumulation rather than erosion during the Cambro-Ordovician period (Avigad *et al.* 2012; Garfunkel, 2015). The West African Craton, the Sahara Metacraton and the Arabian–Nubian Shield are still largely covered by Cambro-Ordovician sedimentary rocks and, therefore, are unlikely to be significant source regions during the Cambro-Ordovician period. We avoid this gap in information and constrain the pre-Variscan palaeogeographic position of Variscan units on the Peri-Gondwanan shelf by comparing the detrital zircon age spectra of the corresponding sedimentary rocks with coevally deposited sedimentary rocks covering the cratonic Gondwana basement (Fig. 3). Similarities to these age distributions either indicate a proximate palaeogeographic position or at least the transport of the zircons by a common delta-fan system.

4. Results

4.a. MDS and clustering results and validation

The MDS of pre-Variscan metasedimentary rocks shows several groups with slightly scattered samples (Fig. 4). HDBSCAN is then the most suited analysis tool for such a slightly noisy distribution of MDS data. Results of the density-based clustering are summarized in Table S5 and Figure S6 in the online Supplementary Material available at http://journals.cambridge.org. HDBSCAN detects four clusters and several outlier samples, i.e. samples with undeterminable provenance or exotic age spectra. The different groups are named according to the provenance of included reference samples (Fig. 4).

The large cluster '4' contains reference samples from northern Africa. Although the cluster contains reference samples from three different regions (West African Craton, Sahara Metacraton and Arabian–Nubian Shield cover sequences), the high density of the clusters indicates a transition among the age spectra of the Peri-Gondwanan shelf sediments. This may be due to mixing of source fingerprints in the age spectra because of sediment mixing or recycling processes during source-to-sink transport.

To cluster the high-density data, agglomerative hierarchical clustering was applied to the northern African group (Fig. 5). The number of clusters is estimated using the gap statistics, yielding discrimination of the northern African group into three clusters (Fig. 5c). The clusters are correlated with reference samples covering the West African Craton, Sahara Metacraton and the Arabian–Nubian Shield. Finally, the clustering result is validated and optimized using the silhouette width (Fig. 5d). The average silhouette width of 0.43 points to an appropriate clustering result. Branches of the dendrogram with low or negative silhouette widths are lastly assigned to the corresponding cluster group of the proposed neighbour (Fig. 5e). Results of the hierarchical clustering are summarized in Table S7 and displayed in Figure S8 in the online Supplementary Material available at http://journals.cambridge.org.

The cluster-coupled MDS gives clusters containing discrete reference samples. Hence, the unsupervised statistical approach allows the identification of the end-member detrital composition of the pre-Variscan sedimentary rocks. The statistical robustness of such a solution is evaluated by the excess scatter of the non-metric MDS output. The goodness-of-fit measure of a non-metric MDS is given by normalizing the raw stress to the sum of the squared fitted distances (Kruskal, 1964; Kruskal & Wish, 1978). The resulting stress value (S value) depends on the sample size of the input dataset and the dimensionality of the MDS configuration. The higher the sample size, the higher the probability of including different clusters of age distributions and/or erroneous data and, thus, the higher the scatter of the MDS configuration. A large sample size and the likely inclusion of age spectra that contain undetected age populations due to insufficiently dated grains, however, characterize the stress factor as representing a noise-value rather than a goodness-of-fit value (Borg & Groenen, 2005). Our MDS solution gives a final stress value of $S = 0.06$ that qualifies the configuration as being 'fair' according to Kruskal (1964). However,

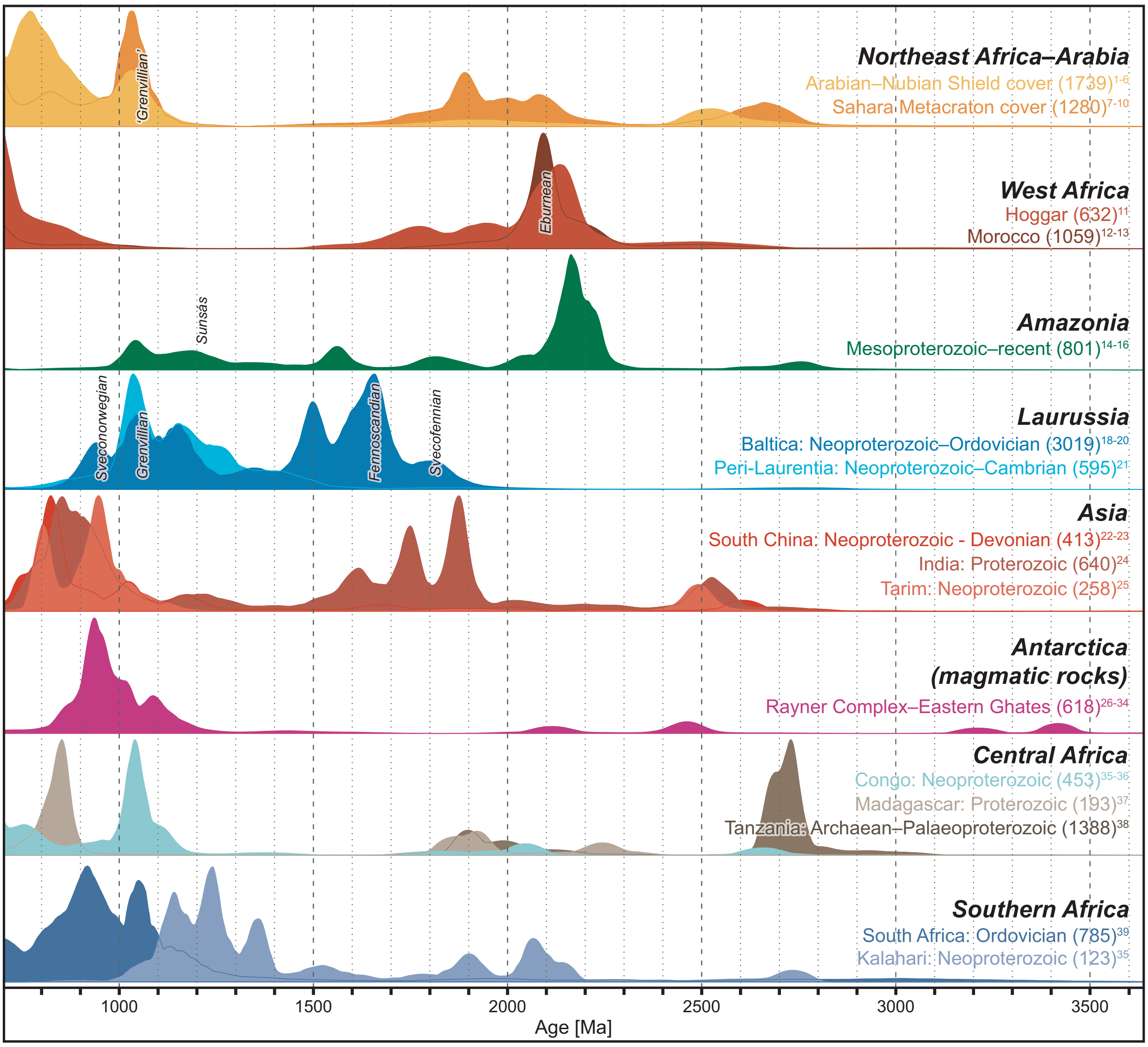

Figure 3. (Colour online) U–Pb ages of detrital zircons of potential source areas. Only pre-Devonian sedimentary rocks unless otherwise specified. Distributions of detrital zircon ages are plotted as kernel density estimates (bandwidth of 20 Ma, Epanechnikov kernel, 90–105 % concordance). Number of analysed ages in brackets. References (superscript): (1) Andresen *et al.* (2014); (2) Avigad *et al.* (2003); (3) Avigad *et al.* (2007); (4) Avigad *et al.* (2015); (5) Kolodner *et al.* (2006); (6) Moghadam *et al.* (2017); (7) Altumi *et al.* (2013); (8) Bea *et al.* (2010); (9) Meinhold *et al.* (2011); (10) Meinhold, Morton & Avigad (2013); (11) Linnemann *et al.* (2011); (12) Abati *et al.* (2010); (13) Avigad *et al.* (2012); (14) Horbe *et al.* (2013); (15) Matteini *et al.* (2012); (16) Andersen, Griffin & Pearson (2002); (17) Be'eri-Shlevin *et al.* (2011); (18) Gee *et al.* (2014); (19) Slama (2016); (20) Bream *et al.* (2004); (21) Hofmann *et al.* (2011); (22) Yao *et al.* (2012); (23) Shu *et al.* (2011); (24) Boger *et al.* (2000); (25) Carson *et al.* (2000); (26) Corvino *et al.* (2005); (27) Corvino & Henjes-Kunst (2007); (28) Corvino *et al.* (2008); (29) Halpin *et al.* (2012); (30) Kelly, Clarke & Fanning (2002); (31) Kelly, Clarke & Fanning (2004); (32) Mikhalsky *et al.* (2006).

regarding the large input sample size of our dataset (n = 227), a value of 0.06 indicates a very robust statistical solution. The statistical analysis of the detrital zircon ages distinguishes four zircon provinces containing significantly different age spectra: (i) Laurussian (with Baltica and Laurentia), (ii) Avalonian, (iii) West African and (iv) East African–Arabian age spectra (Fig. S9 in the online Supplementary Material available at http://journals.cambridge.org).

4.b. Laurussian Zircon Province

The MDS configuration of Laurussian age spectra displays a continuous elliptic group of two clusters containing Baltica- (HDBSCAN cluster '2') and Laurentia-derived samples ('1', Fig. 4). The age spectra of samples from the 'Laurussian Zircon Province' are characterized by Meso- to Palaeoproterozoic zircon crystals with major age peaks at 0.95 Ga (Sveconorwegian event), 1.05–1.15 Ga, 1.5–1.65 Ga (Fennoscandian) and 1.8 Ga (Svecofennian) and minor Neoarchaean populations.

4.c. Avalonian Zircon Province

The MDS configuration of Avalonian age spectra comprises cluster '3' and surrounding outlier samples (Fig. 4) from NW Svalbard, the Avalonian Terranes

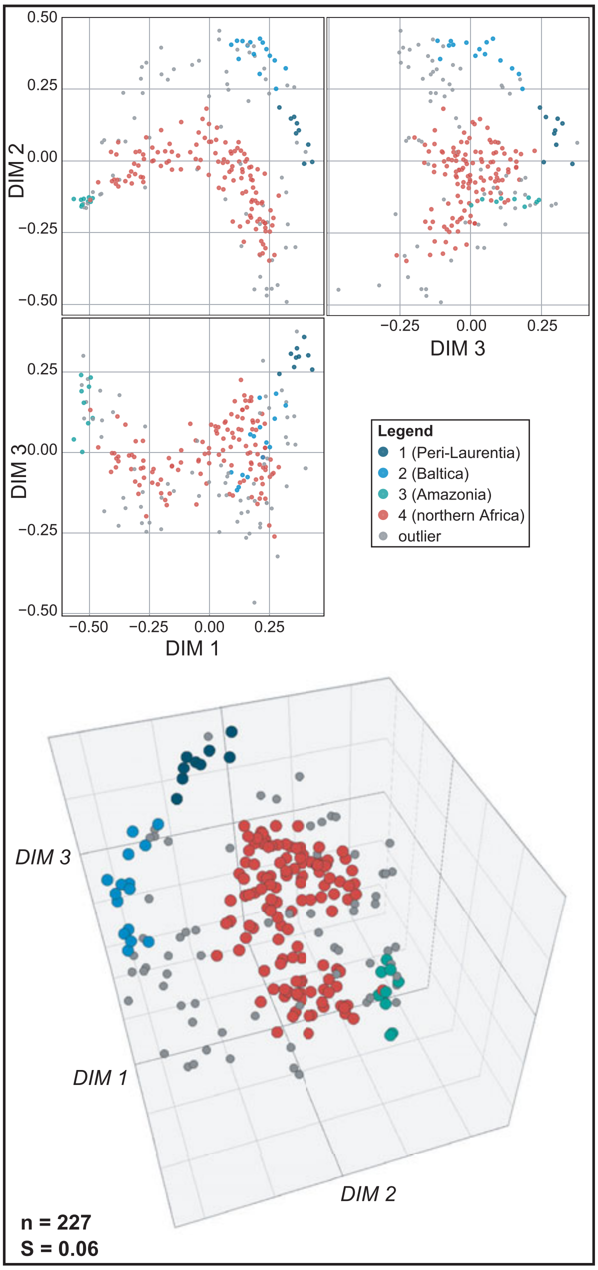

Figure 4. (Colour online) Non-metric multidimensional scaling of >400 Ma metasedimentary rocks (based on calculated Kolmogorov–Smirnov distances between zircon U–Pb age spectra, only zircon ages older than 700 Ma, 90–105 % concordance, minimum 30 ages). n – number of samples used for the statistics; S – stress factor. Colour coding refers to the HDBSCAN results. Minimum points within a cluster = 3. The large cluster '4' (red), i.e. northern Africa/Arabia, is additionally hierarchically clustered in Figure 5. For an interactive three-dimensional version see Figure S6 in the online Supplementary Material available at http://journals.cambridge.org.

of the Appalachians (Ganderia, West Avalonia and Meguma), the British Isles, the Rhenish Massif, the Harz Mountains, the Moravo-Silesian Zone, the Serbo-Macedonian Massif, Pelagonia, the Istanbul Zone, the Mauretanides and northern Morocco. The age patterns of Avalonia are characterized by containing predominantly Mesoproterozoic zircon populations with dominant 1.2 Ga (Sunsás event), ∼1.5 Ga and 2.1–2.2 Ga peaks (Fig. 3) corresponding to an Amazonian signature (Matteini *et al.* 2012; Horbe *et al.* 2013). Significant signatures of the West African cover sequences (Fig. 3) in areas of generally Amazonian predominance (Meguma, North Wales and northern Morocco) indicate deposition at the distal parts of Avalonia (Waldron *et al.* 2011).

The mixing line between Amazonian and Laurussian provenances in the MDS configuration (Fig. S9 in the online Supplementary Material available at http://journals.cambridge.org) points to sediment recycling processes. Laurussian affinities of the Upper Silurian – Lower Devonian samples (Svalbard and Rheno-Hercynian Zone) are related to the proximity of Laurussia after the closure of the Iapetus Ocean (Pettersson, Pease & Frei, 2010; Zeh & Gerdes, 2010), whereas Amazonian ages in Silurian and younger sedimentary rocks point to the recycling of the underlying sedimentary rocks.

4.d. West African Zircon Province

The 'West African Zircon Province' stems from the HDBSCAN cluster '3' (Fig. 4) and the West African cluster of the hierarchical clustering (Fig. 5). The age spectra are characterized by the Eburnean (2.1 Ga) peak, and a 1.8–2.0 Ga peak, whereas 'Grenvillian' (1.0 Ga) zircons are absent. This age distribution corresponds to Precambrian–Lower Palaeozoic (meta-) sedimentary rocks covering the West African Craton in Morocco and Algeria (Abati *et al.* 2010; Linnemann *et al.* 2011; Avigad *et al.* 2012). The West African province comprises sedimentary rocks from the Saxo-Thuringian Zone in the Bohemian Massif and the Sudetes, the Teplá-Barrandian Unit, the Moldanubian Zone, the northern and central parts of the Armorican Massif, the NW French Massif Central, as well as the allochthonous units of the Galicia–Trás-os-Montes Zone and the Ossa-Morena Zone.

The gradual transition of the West African cluster towards the Amazonian cluster (reference samples from NE Brazil and the Damara orogen, Fig. S9 in the online Supplementary Material available at http://journals.cambridge.org), i.e. Amazonian zircons in parts of the West African group (allochthonous units of Galicia–Trás-os-Montes Zone and Ossa-Morena Zone), indicates sediment mixing of material derived from South America and western to central Africa on the Gondwanan shelf.

Because zircon age patterns of the samples assigned to the West African Zircon Province do not change during the entire Early Palaeozoic era, the zircon provenance of sediments remains constant during the investigated time range. There is, however, a temporary change to East African–Arabian age spectra in Upper Ordovician samples.

4.e. East African–Arabian Zircon Province

Zircon age spectra that are dominated by a 1.8–2.0 Ga peak, a subordinate Eburnean (2.1 Ga) peak, a modest 2.5–2.7 Ga peak, a significant ~1.0 Ga 'Grenvillian' peak and a ~800 Ma peak are assigned to the 'East African–Arabian Zircon Province' because of close similarities to sedimentary rocks from Egypt, Israel, Jordan and Iran (Fig. 5). The group comprises sedimentary rocks from the Central Iberian, Cantabrian and West Asturian–Leonese zones, the Pyrenees, Sardinia, Tuscany, Apulia, Sicily, the Southern Alps, the Austroalpine basement of the Alps (Heinrichs *et al.* 2012), the Peloponnese, Crete and the Menderes Massif. Moreover, the province contains samples from South China, the Tarim Block, Madagascar and South Africa. Similarly to the West African Zircon Province, the age patterns of the sedimentary rocks assigned to the East African–Arabian Zircon Province do not change during the entire Early Palaeozoic era, pointing to a constant zircon provenance during the entire time span.

4.f. Exotic age spectra

Individual samples from Pelagonia (Zlatkin, Avigad & Gerdes, 2014), the Brabant Massif (Linnemann *et al.* 2012), the Moravo-Silesian Zone (Košler *et al.* 2014) and the Sudetes (Mazur *et al.* 2012) were not assigned to one of the zircon provinces. Although a sufficiently large number of zircon grains were dated, zircon ages characteristic for a particular province were missing. This may be due to recycling or sediment mixing with an unknown source during the source-to-sink transport. This process affects only four samples and, therefore, may be a rare phenomenon. Samples from other Gondwana areas (North China, basement of Lesser Himalaya, Madagascar, southern Africa and Congo) constitute isolated clusters with no affinities to any sample from the Variscan basement. It is worth noting that all different source reference samples plot in individual

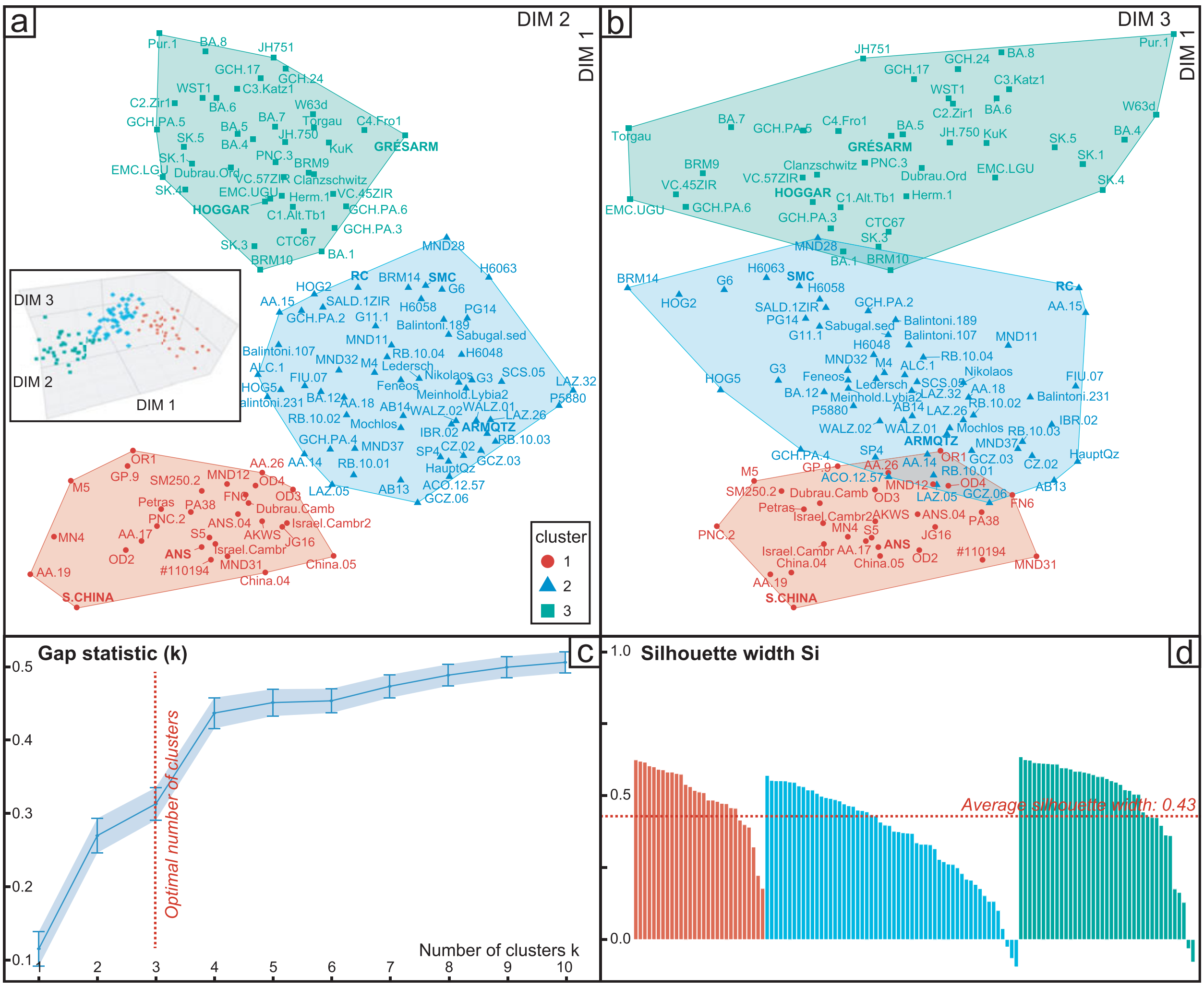

Figure 5. (Colour online) (a–b) Non-metric multidimensional scaling and hierarchical clustering of the 'northern Africa' cluster (Fig. 4). Inset displays the three-dimensional MDS (see Fig. S8 in the online Supplementary Material available at http://journals.cambridge.org). (c) Determination of the optimal number of clusters via gap statistics. (d) Validation of the clustering results based on cluster silhouette plots. The average silhouette $Si = 0.44$ indicates an 'appropriate' clustering (according to Rousseeuw, 1987). Low or negative Si values indicate poor clustering or false cluster assignment (see Table S7 in the online Supplementary Material available at http://journals.cambridge.org).

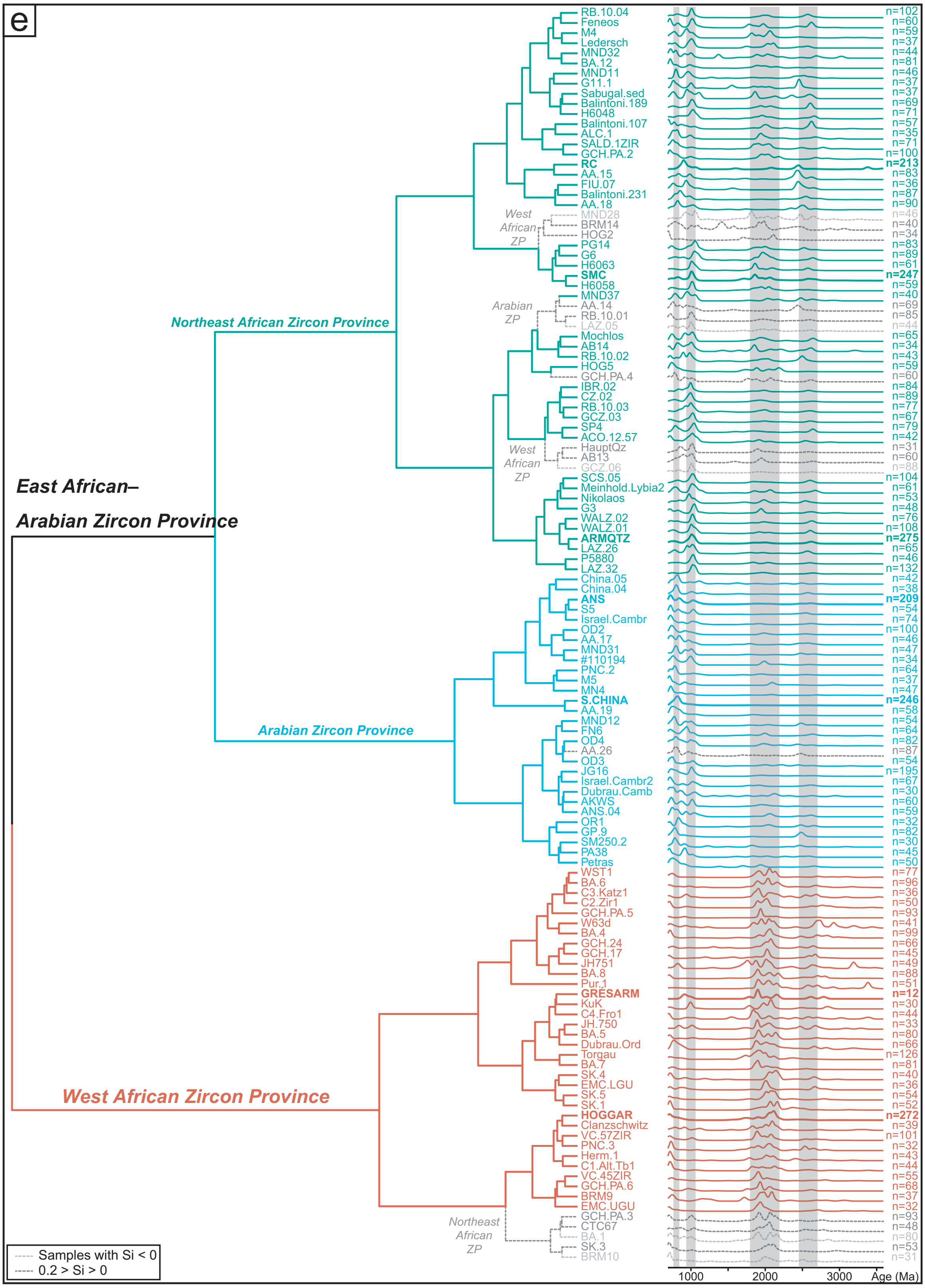

Figure 5. (Continued) (Colour online) (e) Dendrogram of the hierarchical clustering and kernel density estimates of each sample with a bandwidth of 30 Ma, Epanechnikov kernel. *n* refers to the number of concordant zircon grains. Samples with low *Si* values are displayed with grey dotted lines. Samples in bold refer to the compiled reference samples (Fig. 3).

clusters that do not interfinger with clusters of a different source. This indicates that our statistical approach including a huge dataset and targeted filtering is able to identify provenance end-member populations for a composite crust.

5. Discussion

5.a. Evidence for a vast and contiguous Peri-Gondwanan shelf

As demonstrated above, the different zircon provinces can be used to subdivide the pre-orogenic crust of Peri-Gondwana into domains of contrasting provenance. Subsequently these domains were affected by collisional and extensional tectonic processes during the formation and destruction of Pangaea in the Palaeozoic and the Meso- to Cenozoic era, respectively. The extra-Alpine part of Central and Western Europe, i.e. the classic Variscides, preserves the Late Palaeozoic arrangement of these continental crustal domains, whereas the Peri-Gondwanan domains in the Mediterranean region additionally were affected by rifting processes related to the break-up of Pangaea and accretion processes due to later plate convergence between Africa–Arabia and Eurasia during the Alpine orogenic cycle. Although it is out of the scope of this paper to reconstruct the different continental blocks of the Mediterranean region in terms of a pre-break-up, i.e. Pangaea constellation, the dataset allows for testing assumptions about the principal arrangement of the Peri-Gondwanan crustal domains during the Palaeozoic era as well as the number of Palaeozoic oceans.

Our data analysis reveals that the majority of the Peri-Gondwanan crust stays connected with Gondwana until the Early Devonian epoch. Apart from the opening of the Rheic Ocean, which separates Avalonia from mainland Gondwana, there is no evidence for sea floor spreading inside Peri-Gondwana changing the provenance pattern of the sediments. Moreover, the sporadic mixture of West African zircon spectra with East African–Arabian spectra in the East African–Arabian Zircon Province dominated area (e.g. Franz *et al.* 2013; Rösel *et al.* 2014) or vice versa (e.g. Fernández-Suárez *et al.* 2014) indicates sediment exchange between parts of both provinces (as indicated by the mixing line between both end-members, Fig. 4), and thus, rather contradicts the existence of additional oceanic lithosphere.

5.b. The Avalonia Zircon Province north of the Rheic suture

The dataset analysed here further corroborates existing views in terms of Avalonia as a contiguous terrane assembled to Laurussia in the Ordovician–Silurian period (e.g. Murphy *et al.* 2000; Oczlon, Seghedi & Carrigan, 2007; Strachan *et al.* 2007; Satkoski, Barr & Samson, 2010; Ustaömer *et al.* 2011; Barr *et al.* 2012; Willner *et al.* 2013). Peri-Gondwanan crust ascribed to Avalonia (Fig. 2) is characterized by a significant change in the detrital zircon age spectra of Cambrian to Silurian sedimentary rocks, reflecting the change of source areas with the opening of the Rheic Ocean. Pre-Silurian rocks are dominated by detrital age spectra with an Amazonian signature (Fig. 1). The characteristic Baltica–Laurentia detritus in Silurian and younger sedimentary rocks reflects a Laurussian drainage system. Amazonian signatures in sedimentary rocks deposited at this time originate from the recycling of older sedimentary rocks. The Early Palaeozoic separation of Avalonia and related terranes from Gondwana is corroborated by palaeogeographic proxies such as the exclusive occurrence of Ordovician manganese-coticules and the absence of Hirnantian diamictites that are typical for Peri-Gondwanan crust to the south of the Rheic Ocean (Table 1; Fig. 6).

The Meguma terrane contains an Amazonian signature (Fig. 3) with an Eburnean age population, i.e. West African zircons (Murphy *et al.* 2004*a*; Waldron *et al.* 2011). This far travelled West African detritus in the pre-rifting basement is explained by a mixing of Amazonian with West African zircons at the distal shelf position along the Avalonian Peri-Gondwanan shelf (Romer, Kirsch & Kroner, 2011).

The exotic position of Avalonian crust in the Mediterranean, i.e. Pelagonia (Hellenides) and the Serbo-Macedonian Massif (Meinhold *et al.* 2010; Zlatkin, Avigad & Gerdes, 2014, 2017), is corroborated by our data analysis. Both units are sandwiched between crusts of predominantly East African–Arabian provenance. Whether the juxtaposition of these exotic units resulted from pre-Pangaean processes (Zlatkin, Avigad & Gerdes, 2017) or is related to younger tectonics remains an open question and cannot be answered by detrital zircon provenance alone.

5.c. The Peri-Gondwanan shelf south of the Rheic Ocean

5.c.1. The East African–Arabian Zircon Province

The East African–Arabian Zircon Province contains sedimentary rocks from the eastern Gondwana mainland (East Africa, Arabia, Madagascar, South Africa, South China, see Fig. S9 in the online Supplementary Material available at http://journals.cambridge.org). Because the provenance of these samples is still unknown (Collins, Kinny & Razakamanana, 2012; Yao *et al.* 2012; Vorster *et al.* 2015) and detrital zircon age data alone cannot identify the distinct provenance, it is out of scope of this paper to clarify the provenance of the zircon provinces of the northern Peri-Gondwanan shelf. Nevertheless, the Peri-Gondwanan shelf sediments were probably fed by a complex, eastern Gondwana super-fan system with detritus probably from recycled orogens like the East African Orogen, the Rayner–Eastern Ghates Complex and the Irumide Belt (Squire *et al.* 2006; Meinhold, Morton & Avigad, 2013; Rösel *et al.* 2014).

Table 1. Provenance features of crustal blocks from the Acadian–Variscan orogenic belts of Europe

Feature		Avalonian Zircon Province [c]	West African Zircon Province [c]	East African–Arabian Zircon Province [c]
Age pattern of detrital zircon		*Mesoproterozoic zircon populations.	* weak 2.5–2.7 Ga peak, * significant 2.1 Ga Eburnean peak * 1.8 peak, * no ~1 Ga ('Grenvillian') ages * no ~800 Ma peak.	* modest 2.5–2.7 Ga peak, * subordinate 2.1 Ga (Eburnean) peak, * 1.9–2.0 Ga peak, * significant ~1.0 Ga ('Grenvillian') peak, * ~800 Ma peak.
Hirnantian glaciation		* No tillites known, * Local erosional gaps or changes in the sedimentary facies (1).	* Up to several hundred metres thick marine tillites with dropstones; known from the shelf sequences of Saxo-Thuringia, Armorica, Morocco (1, 2, 3, 4, 5).	* Up to several hundred metre thick marine tillites with dropstones; known from the shelf sequences of Iberia, Sardinia and the Carnic Alps. In Saharan Africa mainly known from terrigenous deposits and glacial striation on polished surfaces (2, 3, 4).
Coticules [a]		* Present as coticule- and Mn-carphiolite-bearing layers in Nova Scotia, Ireland, Isle of Man, Wales, the Ardennes, and the Harz Mts., as well as possibly in the Ossa-Morena Zone in form of units with abundant Mn-minerals (6, 7, 8, 9, 10).	Not known (10, 11).	Not known (10, 11).
'Sardic' phase [b]		Not known.	Not known.	* 457–443 Ma tectonic-metamorphic overprint in pre-Variscan basement of the Carnic Alps (12, 13), Agordo basement of the Southern Alps (14), * Middle Ordovician unconformity or hiatus in sedimentary sequences of Montagne Noire (15), Mouthoumet Massif (16), Eastern Pyrenees (17), Central Iberian Zone (18, 19, 20), Sardinia (21), Corsica (22), Sicily (23, 24), in parts of the Carpathians and in southern Turkey (25, 26), Arabian plate (27). * Echoes of the Sardic phase possibly in Darriwilian oolitic ironbeds in West Asturian–Leonese Zone, Cantabrian Zone and southern Central Iberian Zone (28 and references therein).
Phanerozoic tin, tungsten and tantalum mineralizations		* Syn-orogenic (395–380 Ma) in Nova Scotia and New Brunswick, * Post-orogenic (300–275 Ma) in New England states, Cornwall and Ireland (29 and references therein).	Syn-orogenic (340–300 Ma) in * Galicia–Trás-os-Montes Zone, * French Massif Central, * Armorican Massif, * Vosges and Schwarzwald, * Bohemian Massif (29 and references therein).	* 530 Ma LCT-type pegmatites in Ethiopia, Somalia and Oman (30).
Classic zonation of the Variscan orogen	Kossmat (1927), Franke (1989)	* Subvariscan Zone, * Rheno-Hercynian Zone, * Moravo-Silesian Zone (incl. Bruno-Vistulian Zone).	* Saxo-Thuringian Zone, * Teplá-Barrandian Zone, * Moldanubian Zone *sensu stricto*.	
	Lotze (1945), Julivert *et al.* (1972)	* South Portugal Zone.	* Allochthonous Sequences of the Central Iberian Zone (Galicia–Trás-os-Montes Zone), * Ossa-Morena Zone.	* Autochthonous Sequences of the Central Iberian Zone, * West Asturian–Leonese Zone, * Cantabrian Zone.

[a]Ordovician manganese-rich sedimentary rocks. [b]Middle Ordovician. [c]References: (1) Le Heron *et al.* (2007); (2) Robardet & Doré (1988); (3) Villas *et al.* (2002); (4) Monod *et al.* (2003); (5) Linnemann *et al.* (2010*b*); (6) Kramm (1976); (7) Jimenez Millan & Velilla (1998); (8) Kennan & Morris (1999); (9) Waldron *et al.* (2009); (10) Romer, Kirsch & Kroner (2011); (11) Dill *et al.* (2008); (12) Franz & Romer (2007); (13) Zurbriggen (2015); (14) Poli & Zanferrari (1992); (15) Robardet *et al.* (1994); (16) Javier Álvaro *et al.* (2016); (17) Gil Ibarguchi, Navidad & Ortega (1990); (18) Lotze (1956); (19) Gutiérrez-Marco, De San José & Pieren (1990); (20) Valverde-Vaquero & Dunning (2000); (21) Carmignani *et al.* (1982); (22) Rossi, Oggiano & Cocherie (2009); (23) Trombetta *et al.* (2004); (24) Cocco & Funedda (2017); (25) Hammann (1992); (26) Ghienne *et al.* (2010); (27) Sharland *et al.* (2001); (28) Gutiérrez-Marco *et al.* (2002); (29) Romer & Kroner (2015); (30) Küster *et al.* (2009).

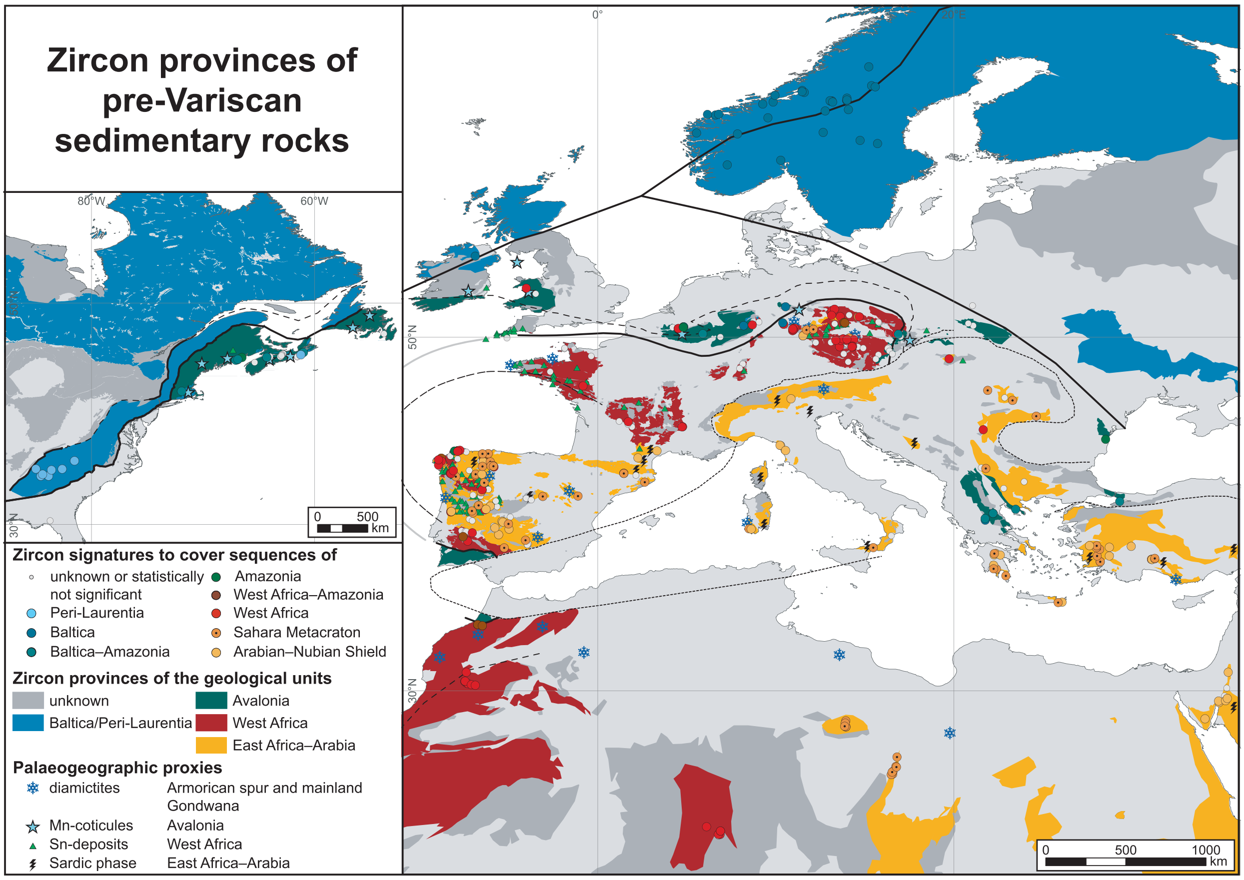

Figure 6. (Colour online) Spatial distribution of the pre-Variscan zircon provinces along the Variscan basement of Europe and North America.

As revealed by our analysis, the East African–Arabian Zircon Province spans from Western Europe to the Middle East (Fig. 6). Zircon data indicating an East African–Arabian provenance previously were only used for regional reconstructions. For instance, relying on the detrital record of the Romanian Carpathians, Balintoni *et al.* (2009) suggested for the ‘Romanian Carpathians Terrane’ a palaeogeographic position close to the Arabian–Nubian Shield. Palaeontological evidence, detrital U–Pb ages and isotopic signatures (Bea *et al.* 2010; Díez Fernández *et al.* 2010; Fernández-Suárez *et al.* 2014; Shaw *et al.* 2014; Orejana *et al.* 2015; Henderson *et al.* 2016) from the Central Iberian, West Asturian–Leonese and Cantabrian zones point to an initial position close to Egypt contradicting classic palaeogeographic models (e.g. Crowley *et al.* 2000; Robardet, 2002; Stampfli, von Raumer & Borel, 2002; von Raumer, Stampfli & Bussy, 2003; Murphy *et al.* 2004*b*; Cocks & Torsvik, 2006; Franke, Cocks & Torsvik, 2017) that all assume a West African provenance (Fig. 1) for this part of Iberia.

Recognizing the vast spatial distribution of this type of Peri-Gondwanan crust, Dörr *et al.* (2015) combined different domains, including North Iberia, Sardinia, Apulia, the Hellenides and Pontides and referred to them as the ‘Minoan Terrane Assemblage’. As visualized in Figure 6, the spatial distribution of the East African–Arabian provenance actually is even larger and reaches at least as far to the east as Iran (Moghadam *et al.* 2017), possibly as far as Tarim and South China. Our data analysis (Fig. 5) reveals that the zircon spectra of Tarim and South China also have close similarities to terranes of the East African–Arabian provenance, which implies that this zircon province encompasses a huge segment of contiguous Peri-Gondwana with comparable provenance. The extent of the East African–Arabian Zircon Province to the east is not well constrained, whereas to the west, i.e. in Western Europe, it is sharply defined, especially in Iberia (see Fig. 6).

5.c.2. The West African Zircon Province

The largest part of the internal zone of the Variscides of Europe and northern Africa *sensu stricto* belongs to the West African Zircon Province. Here, the tectonometamorphic record indicates initial collision between Laurussia and Peri-Gondwana in Lower Devonian rocks at 400 Ma (e.g. Kreuzer *et al.* 1989; Schaltegger *et al.* 1996; Lardeaux *et al.* 2001; Nutman *et al.* 2001; Ordóñez Casado *et al.* 2001; Lucks *et al.* 2002; Kryza & Fanning, 2007; Bröcker *et al.* 2009; Berger *et al.* 2010), whereas continental crust of the East African–Arabian Zircon Province is not affected by collisional tectonics before the Carboniferous period, i.e. *c*. 50 Ma later (Dallmeyer *et al.* 1997; Giacomini, Bomparola & Ghezzo, 2005; Rubatto *et al.* 2010; Langone *et al.* 2011; Martínez Catalán *et al.* 2014). Hence, the West African Zircon Province can be regarded as the leading edge of Peri-Gondwana, i.e. the Armorican Spur (Kroner & Romer, 2013), during the collision of Gondwana and Laurussia.

In terms of the pre-orogenic sedimentary record, Lower Palaeozoic sequences of the West African Zircon Province carry the chemical signal of intense chemical weathering on a stable continent, i.e. decomposition of feldspar with pronounced loss of those feldspar-bound elements (Ca, Na, Sr, Pb) that are not incorporated in or adsorbed on clay minerals. Sedimentary accumulation of this debris on the extended Peri-Gondwanan shelf as a result of break-up and uplift was followed by tectonic stacking during the Variscan collision and subsequent melting, eventually resulting in the formation of major tin–tungsten deposits within the Variscides (Romer & Kroner, 2015, 2016). The lack of notable tin deposits in terranes of the East African–Arabian Zircon Province underlines the significant differences in terms of provenance between the West African Zircon Province and the East African–Arabian Zircon Province (Table 1; Fig. 6).

As revealed by our study, the West African Zircon Province contains detrital age spectra that resemble sedimentary rocks from Morocco, the Hoggar Shield, the Damara orogen and from NE Brazil. Because of the contrasting detrital age spectra, the shelf areas belonging to the West African and East African–Arabian zircon provinces cannot be supplied by a common Gondwana super-fan system. We propose that the northern Peri-Gondwanan shelf was fed by at least two independent fan systems, namely the ‘West Gondwana super-fan system’ and the ‘East Gondwana super-fan system’.

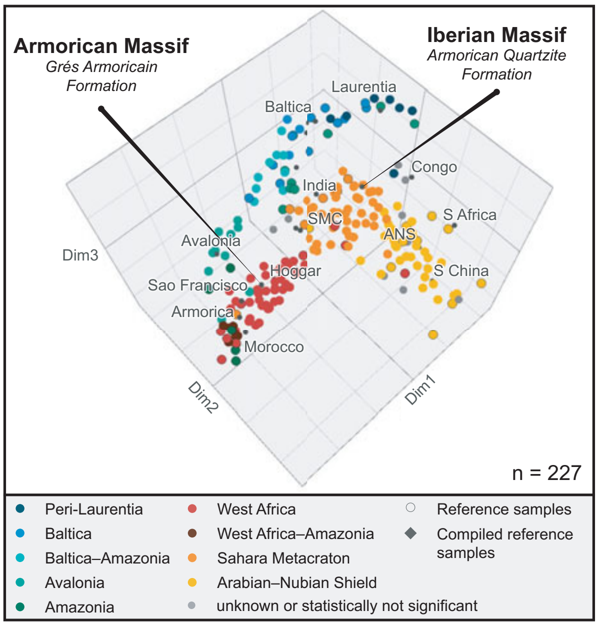

Figure 7. (Colour online) Three-dimensional output of non-metrical MDS and final discrimination of the pre-Variscan samples into the palaeogeographic groups. Note the significantly different age spectra of the Lower Ordovician French ‘Grès Armoricain Formation’ and the Iberian ‘Armorican Quartzite Formation’. Figure S9 in the online Supplementary Material available at http://journals.cambridge.org is interactive and provides additional information about each data point when hovering over it with the mouse cursor.

5.d. The Early Palaeozoic palaeogeography of Iberia

Because of lithological and palaeontological similarities between the Lower Palaeozoic strata of Central Iberia and Armorica (Brittany), most palaeogeographic reconstructions of the pre-Variscan Gondwanan architecture place Iberia adjacent to Armorica. For instance, lithostratigraphic arguments led to the classic correlation of autochthonous Lower Ordovician quartzites of the ‘Grès Armoricain Formation’ and the ‘Armorican Quartzite Formation’ of Brittany and Central Iberia, respectively. This correlation served as a strong argument for spatial closeness in the Early Palaeozoic era. Palaeomagnetic studies are not able to prove this hypothesis since reliable data are lacking due to large gaps in the geological record of Iberia and the Armorican Massif (Perroud & Bonhommet, 1984; Perroud, Calza & Khattach, 1991; Tait *et al.* 1997; Franke, Cocks & Torsvik, 2017).

Our statistical evaluation yields significantly different zircon spectra for Iberia and the Armorican Massif, especially for the Armorican Quartzite and the Grès Armoricain formations (Fig. 7). A different palaeogeographic position is additionally corroborated by the East African faunal affinities of Central Iberia in contrast to the West African affinities of Brittany (e.g. Mélou, Oulebsir & Paris, 1999; Gutiérrez-Marco *et al.* 2002; Robardet & Gutiérrez-Marco, 2002). Hence, in terms of sediment supply, the coeval depositional areas are unrelated and there may be a large distance between Armorica and Central Iberia before rifting of Peri-Gondwana started.

In terms of deformation and metamorphic ages, the Armorican Massif and Central Iberia were differently affected by the Variscan orogeny. The Armorican Massif was affected by the early Variscan tectono-metamorphic event in the Early Devonian epoch (Ballèvre *et al.* 1994; Rolet *et al.* 1994; Kroner & Romer, 2013), whereas Central Iberia remained in a stable shelf position with undisturbed marine sedimentation at this time (Garcia-Alcalde *et al.* 2002). Thus, the regions of the West African Zircon Province should be located close to West Africa, whereas Central Iberia and other regions of the East African–Arabian Zircon Province may have been positioned on the Peri-Gondwanan shelf further east, i.e. adjacent to the Sahara Metacraton and the Arabian–Nubian Shield (see also discussion in Meinhold, Morton & Avigad, 2013). The resulting late Variscan westward-directed lateral escape of Iberia is in many models not considered (e.g. Matte, 2001; Franke, Cocks &

Torsvik, 2017) or underestimated (Kroner & Romer, 2013).

5.e. Palaeogeographic models

The provenance pattern of the Variscan orogen and its palaeogeographic implications are not regarded in any tectonic model. The crucial point is the pre-orogenic position of Iberia. Instead of an East African–Arabian provenance, Iberia is commonly believed to have a West African provenance and, thus, is located close to the West African Craton in many models (Matte, 2001; Kroner & Romer, 2013; Franke, Cocks & Torsvik, 2017; Fig. 2).

Stampfli *et al.* (2013) considered an eastern position of Central Iberia, which is supported by palaeontological data (e.g. Mélou, Oulebsir & Paris, 1999; Gutiérrez-Marco *et al.* 2002; Robardet & Gutiérrez-Marco, 2002) and in line with our provenance analysis that indicates that Iberia is part of the East African–Arabian Zircon Province (Fig. 1d). Stampfli *et al.* (2013) placed Iberia with the Moldanubian Zone and the French Massif Central in the eastern part of the proposed Galatian Superterrane, even though the latter two regions show a completely different provenance, i.e. the West African Zircon Province. Moreover, the classic Avalonian terranes of the Northern Appalachians, in particular Meguma and Brunswick, and parts of Far East Avalonia, i.e. Dobrogea, Moesia and the Istanbul Zone are also interpreted as integral parts of the Galatian Superterrane that supposedly did not detach from Gondwana before the Devonian period (Fig. 1d). This palaeogeographic reconstruction, however, is in conflict with the palaeontological and sedimentary record (Boyce, Ash & O'Brien, 1991; Williams, 1993; Dean *et al.* 2000; Chen *et al.* 2002; Oczlon, Seghedi & Carrigan, 2007; Pollock, Hibbard & van Staal, 2011) and provenance data (this study) of these areas showing Avalonian and Laurussian affinities since the Silurian period. Hence, the Galatian Superterrane represents an unconstrained assemblage of Peri-Gondwanan crust with apparently randomly juxtaposed domains of the Avalonian, West African and East African–Arabian zircon provinces. Such a zircon provenance pattern would imply that the transport agents (e.g. rivers) would cross.

6. Conclusions

Multidimensional scaling coupled with density-based clustering allows the identification of provenance end-member populations of the composite Variscan crust. The resulting pre-orogenic palaeogeographic constraints should be considered in future plate tectonic models:

The discrimination of the pre-Pangaean continental crust into four principal zircon provinces, namely the Laurussian, the Avalonian, the West African and the East African–Arabian zircon provinces, and their spatial distribution provide fundamental constraints that are tested against published tectonic models, litho-biostratigraphic correlations among different terranes and palaeogeographic reconstructions of Peri-Gondwana:

(i) The Avalonian Zircon Province constitutes the contiguous Avalonian part of the Peri-Gondwanan shelf that has received sediments derived from the Amazonas Craton, and, after the separation from Gondwana, sediments derived from Laurussia.

(ii) The East African–Arabian Zircon Province characterizes the large contiguous Peri-Gondwanan shelf from Central Iberia to Tarim and has received detritus via the eastern Gondwana super-fan system.

(iii) The West African Zircon Province constitutes part of the shelf adjacent to the West African Craton and the ultimate leading edge of Gondwana during the collision with Laurussia, i.e. the Armorican Spur. The detritus was shed by the western Gondwana super-fan system.

(iv) The collision of the Armorican Spur is followed by the westward indention of the Iberian promontory by late Variscan lateral escape movements. This juxtaposes sedimentary rocks of the West African Zircon Province (Armorican Spur) with sedimentary rocks of the East African–Arabian Zircon Province (Iberia).

(v) The zonation of the zircon provinces overlaps with domain-specific features that provide additional palaeogeographic proxies, namely manganese-coticules representative for the Avalonian Zircon Province, the Sardic tectono-metamorphic event for the East African–Arabian Zircon Province and tin–tungsten deposits for the West African Zircon Province.

(vi) The statistical analysis of the detrital zircon ages provides no evidence for the existence of any additional oceans to the south of the Rheic Ocean, separating the zircon provinces of the Peri-Gondwanan crust from each other or from the Gondwana mainland. The pre-Pangaean architecture of the Peri-Gondwanan crust is explained by an extended but contiguous Gondwanan shelf. Nevertheless, the Sardic tectono-metamorphic event at the western edge of the East African–Arabian Zircon Province indicates intracontinental tectonics probably related to plate tectonic reorganization due to the ongoing formation of Pangaea.

Acknowledgements. We are grateful to Sonja Frölich and Judy Adamek (Technische Universität Bergakademie Freiberg) for their help to collect the data. Pieter Vermeesch (UCL) is thanked for methodological advice and implementation of very helpful tools in the R's package 'provenance' (Vermeesch, Resentini & Garzanti, 2016). We acknowledge Guido Meinhold for editorial handling. This research was supported by the BMBF r4 project 'GEM' (grant number: 033R134).

Supplementary material

To view supplementary material for this article, please visit https://doi.org/10.1017/S0016756818000031

References

Abati, J., Aghzer, A. M., Gerdes, A. & Ennih, N., 2010. Detrital zircon ages of Neoproterozoic sequences of the Moroccan Anti-Atlas belt. *Precambrian Research* **181**, 115–28.

Altumi, M. M., Elicki, O., Linnemann, U., Hofmann, M., Sagawe, A. & Gärtner, A. 2013. U–Pb LA-ICP-MS detrital zircon ages from the Cambrian of Al Qarqaf Arch, central-western Libya: provenance of the West Gondwanan sand sea at the dawn of the early Palaeozoic. *Journal of African Earth Sciences* **79**, 74–97.

Andersen, T. 2005. Detrital zircons as tracers of sedimentary provenance: limiting conditions from statistics and numerical simulation. *Chemical Geology* **216**, 249–70.

Andersen, T., Griffin, W. L. & Pearson, N. J. 2002. Crustal evolution in the SW part of the Baltic Shield: the Hf isotope evidence. *Journal of Petrology* **43**, 1725–47.

Andersen, T., Kristoffersen, M. & Elburg, M. A. 2016. How far can we trust provenance and crustal evolution information from detrital zircons? A South African case study. *Gondwana Research* **34**, 129–48.

Andresen, A., Abu El-Enen, M. M., Stern, R. J., Wilde, S. A. & Ali, K. A. 2014. The Wadi Zaghra metasediments of Sinai, Egypt: new constraints on the late Cryogenian–Ediacaran tectonic evolution of the northernmost Arabian–Nubian Shield. *International Geology Review* **56**, 1020–38.

Arboit, F., Collins, A. S., Morley, C. K., King, R. & Amrouch, K. 2016. Detrital zircon analysis of the southwest Indochina terrane, central Thailand: unravelling the Indosinian orogeny. *Geological Society of America Bulletin* **128**, 1024–43.

Arndt, N. T. & Goldstein, S. L. 1987. Use and abuse of crust-formation ages. *Geology* **15**, 893–95.

Arthaud, F. & Matte, P. 1977. Late Paleozoic strike-slip faulting in southern Europe and northern Africa: result of a right-lateral shear zone between the Appalachians and the Urals. *Geological Society of America Bulletin* **88**, 1305–20.

Avigad, D., Gerdes, A., Morag, N. & Bechstädt, T. 2012. Coupled U–Pb–Hf of detrital zircons of Cambrian sandstones from Morocco and Sardinia: implications for provenance and Precambrian crustal evolution of North Africa. *Gondwana Research* **21**, 690–703.

Avigad, D., Kolodner, K., McWilliams, M., Persing, H. & Weissbrod, T. 2003. Origin of northern Gondwana Cambrian sandstone revealed by detrital zircon SHRIMP dating. *Geology* **31**, 227–30.

Avigad, D., Sandler, A., Kolodner, K., Stern, R. J., McWilliams, M., Miller, N. & Beyth, M. 2005. Mass-production of Cambro–Ordovician quartz-rich sandstone as a consequence of chemical weathering of Pan-African terranes: environmental implications. *Earth and Planetary Science Letters* **240**, 818–26.

Avigad, D., Stern, R. J., Beyth, M., Miller, N. & McWilliams, M. O. 2007. Detrital zircon U–Pb geochronology of Cryogenian diamictites and Lower Paleozoic sandstone in Ethiopia (Tigrai): age constraints on Neoproterozoic glaciation and crustal evolution of the southern Arabian–Nubian Shield. *Precambrian Research* **154**, 88–106.

Avigad, D., Weissbrod, T., Gerdes, A., Zlatkin, O., Ireland, T. R. & Morag, N. 2015. The detrital zircon U–Pb–Hf fingerprint of the northern Arabian-Nubian Shield as reflected by a Late Ediacaran arkosic wedge (Zenifim Formation; subsurface Israel). *Precambrian Research* **266**, 1–11.

Balintoni, I., Balica, C., Ducea, M. N., Chen, F., Hann, H. P. & Şabliovschi, V. 2009. Late Cambrian–Early Ordovician Gondwanan terranes in the Romanian Carpathians: a zircon U–Pb provenance study. *Gondwana Research* **16**, 119–33.

Ballèvre, M., Le Goff, E. & Hébert, R. 2001. The tectonothermal evolution of the Cadomian belt of northern Brittany, France: a Neoproterozoic volcanic arc. *Tectonophysics* **331**, 19–43.

Ballèvre, M., Marchand, J., Godard, G., Goujou, J.-C., Christian, J. & Wyns, R. 1994. Eo-Hercynian Events in the Armorican Massif. In *Pre-Mesozoic Geology in France and Related Areas* (eds. J. Chantraine, J. Rolet, D. S. Santallier, A. Piqué & J. D. Keppie), pp. 183–94. Berlin, Heidelberg: Springer.

Barr, S. M., Hamilton, M. A., Samson, S. D., Satkoski, A. M. & White, C. E. 2012. Provenance variations in northern Appalachian Avalonia based on detrital zircon age patterns in Ediacaran and Cambrian sedimentary rocks, New Brunswick and Nova Scotia, Canada. *Canadian Journal of Earth Sciences* **49**, 533–46.

Bea, F., Montero, P., Talavera, C., Abu Anbar, M., Scarrow, J. H., Molina, J. F. & Moreno, J. A. 2010. The palaeogeographic position of Central Iberia in Gondwana during the Ordovician: evidence from zircon chronology and Nd isotopes. *Terra Nova* **22**, 341–6.

Bearden, W. O., Sharma, S. & Teel, J. E. 1982. Sample size affects on chi square and other statistics used in evaluating causal models. *Journal of Marketing Research* **19**, 425–30.

Be'eri-Shlevin, Y., Gee, D., Claesson, S., Ladenberger, A., Majka, J., Kirkland, C., Robinson, P. & Frei, D. 2011. Provenance of Neoproterozoic sediments in the Särv nappes (Middle Allochthon) of the Scandinavian Caledonides: LA-ICP-MS and SIMS U–Pb dating of detrital zircons. *Precambrian Research* **187**, 181–200.

Belka, Z., Ahrendt, H., Franke, W. & Wemmer, K. 2000. The Baltica-Gondwana suture in central Europe: evidence from K–Ar ages of detrital muscovites and biogeographical data. In *Orogenic Processes: Quantification and Modelling in the Variscan Belt* (eds W. Franke, R. Altherr, V. Haak, O. Oncken & D. Tanner), pp. 87–102. Geological Society of London, Special Publication no. 179.

Belka, Z. & Narkiewicz, M. 2008. Devonian. In *The Geology of Central Europe. Volume 1: Precambrian and Palaeozoic* (ed. T. McCann), pp. 383–410. London: The Geological Society of London.

Berger, J., Féménias, O., Ohnenstetter, D., Bruguier, O., Plissart, G., Mercier, J.-C. C. & Demaiffe, D. 2010. New occurrence of UHP eclogites in Limousin (French Massif Central): age, tectonic setting and fluid–rock interactions. *Lithos* **118**, 365–82.

Blatt, H. 1967. Provenance determinations and recycling of sediments. *Journal of Sedimentary Petrology* **37**, 1031–44.

Boger, S. D., Carson, C. J., Wilson, C. J. L. & Fanning, C. M. 2000. Neoproterozoic deformation in the Radok Lake region of the northern Prince Charles Mountains, east Antarctica; evidence for a single protracted orogenic event. *Precambrian Research* **104**, 1–24.

Borg, I. & Groenen, P. J. F. 2005. *Modern Multidimensional Scaling: Theory and Applications*, 2nd edition. New York: Springer.

Boyce, W. D., Ash, J. S. & O'Brien, B. H. 1991. A new fossil locality in the Bay of Exploits, central

Newfoundland. *Current Research, Newfoundland Department of Mines and Energy, Geological Survey Branch Report* **91-1**, 79–82.

Braid, J. A., Murphy, J. B., Quesada, C. & Mortensen, J. 2011. Tectonic escape of a crustal fragment during the closure of the Rheic Ocean: U–Pb detrital zircon data from the Late Palaeozoic Pulo do Lobo and South Portuguese zones, southern Iberia. *Journal of the Geological Society, London* **168**, 383–92.

Bream, B. R., Hatcher, R. D., Miller, C. F. & Fullagar, P. D. 2004. Detrital zircon ages and Nd isotopic data from the southern Appalachian crystalline core, Georgia, South Carolina, North Carolina, and Tennessee: new provenance constraints for part of the Laurentian margin. In *Proterozoic Tectonic Evolution of the Grenville Orogen in North America* (eds R. P. Tollo, J. McLelland, L. Corriveau & M. J. Bartholomew), pp. 459–75. Geological Society of America, Memoirs no. 197.

Breitkreuz, C. & Kennedy, A. 1999. Magmatic flare-up at the Carboniferous/Permian boundary in the NE German Basin revealed by SHRIMP zircon ages. *Tectonophysics* **302**, 307–26.

Bröcker, M., Klemd, R., Cosca, M., Brock, W., Larionov, A. N. & Rodionov, N. 2009. The timing of eclogite facies metamorphism and migmatization in the Orlica-Śnieżnik complex, Bohemian Massif: constraints from a multimethod geochronological study. *Journal of Metamorphic Geology* **27**, 385–403.

Campello, R. J. G. B., Moulavi, D. & Sander, J. 2013. Density-based clustering based on hierarchical density estimates. In *Advances in Knowledge Discovery and Data Mining. PAKDD 2013. Lecture Notes in Computer Science* (eds J. Pei, V. S. Tseng, L. Cao, H. Motoda & G. Xu), pp. 160–72. Berlin, Heidelberg: Springer.

Carmignani, L., Franceschelli, M., Pertusati, P. C., Memmi, I. & Ricci, C. A. 1982. An example of compositional control of the celadonitic content of muscovite and the incoming of biotite in metapelites (Nurra, NW Sardinia). *Neues Jahrbuch fur Mineralogie, Monatshefte* **7**, 289–311.

Carson, C. J., Boger, S. D., Fanning, C. M., Wilson, C. J. L. & Thost, D. E. 2000. SHRIMP U–Pb geochronology from Mount Kirkby, northern Prince Charles Mountains, East Antarctica. *Antarctic Science* **12**, 429–42.

Cawood, P. A., Hawkesworth, C. J. & Dhuime, B. 2012. Detrital zircon record and tectonic setting. *Geology* **40**, 875–8.

Cawood, P. A., Hawkesworth, C. J. & Dhuime, B. 2013. The continental record and the generation of continental crust. *Geological Society of America Bulletin* **125**, 14–32.

Chantraine, J., Egal, E., Thiéblemont, D., Le Goff, E., Guerrot, C., Ballèvre, M. & Guennoc, P. 2001. The Cadomian active margin (North Armorican Massif, France): a segment of the North Atlantic Panafrican belt. *Tectonophysics* **331**, 1–18.

Chen, F., Siebel, W., Satir, M., Terzioğlu, M. & Saka, K. 2002. Geochronology of the Karadere basement (NW Turkey) and implications for the geological evolution of the Istanbul zone. *International Journal of Earth Sciences* **91**, 469–81.

Cocco, F. & Funedda, A. 2017. The Sardic Phase: field evidence of Ordovician tectonics in SE Sardinia, Italy. *Geological Magazine*, published online 14 September 2017. doi: 10.1017/s0016756817000723. 14 pp.

Cocks, L. R. M. & Fortey, R. A. 1982. Faunal evidence for oceanic separations in the Palaeozoic of Britain. *Journal of the Geological Society, London* **139**, 465–78.

Cocks, L. R. M., McKerrow, W. S. & Van Staal, C. R. 1997. The margins of Avalonia. *Geological Magazine* **134**, 627–36.

Cocks, L. R. M. & Torsvik, T. H. 2002. Earth geography from 500 to 400 million years ago: a faunal and palaeomagnetic review. *Journal of the Geological Society, London* **159**, 631–44.

Cocks, L. R. M. & Torsvik, T. H. 2006. European geography in a global context from the Vendian to the end of the Palaeozoic. In *European Lithosphere Dynamics* (eds D. G. Gee & R. A. Stephenson), pp. 83–95. The Geological Society of London, Memoirs no. 32.

Collins, A. S., Kinny, P. D. & Razakamanana, T. 2012. Depositional age, provenance and metamorphic age of metasedimentary rocks from southern Madagascar. *Gondwana Research* **21**, 353–61.

Corvino, A. F., Boger, S. D., Henjes-Kunst, F., Wilson, C. J. L. & Fitzsimons, I. C. W. 2008. Superimposed tectonic events at 2450 Ma, 2100 Ma, 900 Ma and 500 Ma in the North Mawson Escarpment, Antarctic Prince Charles Mountains. *Precambrian Research* **167**, 281–302.

Corvino, A. F., Boger, S. D., Wilson, C. J. L. & Fitzsimons, I. C. W. 2005. Geology and SHRIMP U–Pb zircon chronology of the Clemence Massif, central Prince Charles Mountains, East Antarctica. *Terra Antarctica* **12**, 55–68.

Corvino, A. & Henjes-Kunst, F. 2007. A record of 2.5 and 1.1 billion year old crust in the Lawrence Hills, Antarctic Southern Prince Charles Mountains. *Terra Antarctica* **14**, 13.

Crowley, Q. G., Floyd, P. A., Winchester, J. A., Franke, W. & Holland, J. G. 2000. Early Palaeozoic rift-related magmatism in Variscan Europe: fragmentation of the Armorican Terrane Assemblage. *Terra Nova* **12**, 171–80.

Dallmeyer, R. D., Catalán, J. R. M., Arenas, R., Gil Ibarguchi, J. I., Gutiérrez, Alonso, G., Farias, P., Bastida, F. & Aller, J. 1997. Diachronous Variscan tectonothermal activity in the NW Iberian Massif: evidence from $^{40}Ar/^{39}Ar$ dating of regional fabrics. *Tectonophysics* **277**, 307–37.

Dean, W. T., Monod, O., Rickards, R. B., Demir, O. & Bultynck, P. 2000. Lower Palaeozoic stratigraphy and palaeontology, Karadere–Zirze area, Pontus Mountains, northern Turkey. *Geological Magazine* **137**, 555–82.

Dickinson, W. R. & Gehrels, G. E. 2009a. U–Pb ages of detrital zircons in Jurassic eolian and associated sandstones of the Colorado Plateau: evidence for transcontinental dispersal and intraregional recycling of sediment U–Pb ages of detrital zircons in Colorado Plateau eolianites. *Geological Society of America Bulletin* **121**, 408–33.

Dickinson, W. R. & Gehrels, G. E. 2009b. Use of U–Pb ages of detrital zircons to infer maximum depositional ages of strata: a test against a Colorado Plateau Mesozoic database. *Earth and Planetary Science Letters* **288**, 115–25.

Díez Fernández, R., Catalán, J. R. M., Gerdes, A., Abati, J., Arenas, R. & Fernández-Suárez, J. 2010. U–Pb ages of detrital zircons from the Basal allochthonous units of NW Iberia: provenance and paleoposition on the northern margin of Gondwana during the Neoproterozoic and Paleozoic. *Gondwana Research* **18**, 385–99.

DILL, H. G., SACHSENHOFER, R. F., GRECULA, P., SASVÁRI, T., PALINKAŠ, L. A., BOROJEVIC-ŠOŠTARIC, S., STRMIC-PALINKAŠ, S., PROCHASKA, W., GARUTI, G., ZACCARINI, F., ARBOUILLE, D. & H.-M., SCHULZ. 2008. Fossil fuels, ore and industrial minerals. In *The Geology of Central Europe. Volume 1: Precambrian and Palaeozoic* (ed. T. McCann), pp. 1341–449. London: The Geological Society of London.

DÖRR, W., ZULAUF, G., GERDES, A., LAHAYE, Y. & KOWALCZYK, G. 2015. A hidden Tonian basement in the eastern Mediterranean: age constraints from U–Pb data of magmatic and detrital zircons of the External Hellenides (Crete and Peloponnesus). *Precambrian Research* **258**, 83–108.

DUDEK, A. 1995. Moravo-Silesian Zone – metamorphic evolution. In *Pre-Permian Geology of Central and Eastern Europe* (eds R. D. Dallmeyer, W. Franke & K. Weber), pp. 508–11. Berlin: Springer.

DUNNING, G. R., SWINDEN, H. S., KEAN, B. F., EVANS, D. T. W. & JENNER, G. A. 2009. A Cambrian island arc in Iapetus: geochronology and geochemistry of the Lake Ambrose volcanic belt, Newfoundland Appalachians. *Geological Magazine* **128**, 1–17.

ESTER, M., KRIEGEL, H.-P., SANDER, J. & XU, X. 1996. A density-based algorithm for discovering clusters in large spatial databases with noise. *Proceedings of the Second International Conference on Knowledge Discovery and Data Mining (KDD-96)* **96**, 226–31.

EZZOUHAIRI, H., RIBEIRO, M. L., AIT AYAD, N., MOREIRA, M. E., CHARIF, A., RAMOS, J. M. F., DE OLIVEIRA, D. P. S. & COKE, C. 2008. The magmatic evolution at the Moroccan outboard of the West African craton between the Late Neoproterozoic and the Early Palaeozoic. In *The Boundaries of the West African Craton* (eds N. Ennih & J.-P. Liégeois), pp. 329–43. Geological Society of London, Special Publication no. 297.

FEDO, C. M., SIRCOMBE, K. N. & RAINBIRD, R. H. 2003. Detrital zircon analysis of the sedimentary record. *Reviews in Mineralogy and Geochemistry* **53**, 277–303.

FERNÁNDEZ SUÁREZ, J., GUTIÉRREZ ALONSO, G., JENNER, G. A. & TUBRETT, M. N. 1998. Edades del basamento pre-varisco en Iberia: Herencia Icartiense, Grenville y Cadomiense en rocas del Complejo Olio de Sapo (NW de España). Estudio geocronológico mediante ablación láser. *Studia Geologica Salmanticensia* **34**, 103–21.

FERNÁNDEZ-SUÁREZ, J., GUTIÉRREZ-ALONSO, G., PASTOR-GALÁN, D., HOFMANN, M., MURPHY, J. B. & LINNEMANN, U. 2014. The Ediacaran–Early Cambrian detrital zircon record of NW Iberia: possible sources and paleogeographic constraints. *International Journal of Earth Sciences* **103**, 1335–57.

FRANKE, W. 1989. Tectonostratigraphic units in the Variscan belt of central Europe. In *Terranes in the Circum-Atlantic Paleozoic Orogens* (ed. R. D. Dallmeyer), pp. 67–90. Geological Society of America, Special Papers no. 230.

FRANKE, W. 2000. The mid-European segment of the Variscides: tectonostratigraphic units, terrane boundaries and plate tectonic evolution. In *Orogenic Processes: Quantification and Modelling in the Variscan Belt* (eds W. Franke, V. Haak, O. Oncken & D. Tanner), pp. 35–61. Geological Society of London: Special Publication no. 179.

FRANKE, W., COCKS, L. R. M. & TORSVIK, T. H. 2017. The Palaeozoic Variscan oceans revisited. *Gondwana Research* **48**, 257–84.

FRANZ, C., LINNEMANN, U., HOFMANN, M., WINKLER, R. & ULLRICH, B. 2013. U–Pb ages of detrital zircons, fossils, and facies of the Cambro-Ordovician overstep sequence of the eastern Lausitz Block (Dubrau and Ober-Prauske formations, Saxo-Thuringian Zone). *Geologica Saxonica* **59**, 45–63.

FRANZ, L. & ROMER, R. L. 2007. Caledonian high-pressure metamorphism in the Strona-Ceneri Zone (Southern Alps of southern Switzerland and northern Italy). *Swiss Journal of Geosciences* **100**, 457–67.

FRIEDL, G., FINGER, F., MCNAUGHTON, N. J. & FLETCHER, I. R. 2000. Deducing the ancestry of terranes: SHRIMP evidence for South America-derived Gondwana fragments in central Europe. *Geology* **28**, 1035–8.

GARCIA-ALCALDE, J. L., CARLS, P., ALONSO, M. V. P., LÓPEZ, J. S., SOTO, F. T., TRUYOLS-MASSONI, M. & VALENZUELA-RIOS, J. I. 2002. Devonian. In *The Geology of Spain* (eds W. Gibbons & T. Moreno), pp. 67–91. London: Geological Society of London.

GARFUNKEL, Z. 2015. The relations between Gondwana and the adjacent peripheral Cadomian domain—constraints on the origin, history, and paleogeography of the peripheral domain. *Gondwana Research* **28**, 1257–81.

GEE, D. G., LADENBERGER, A., DAHLQVIST, P., MAJKA, J., BE'ERI-SHLEVIN, Y., FREI, D. & THOMSEN, T. 2014. The Baltoscandian margin detrital zircon signatures of the central Scandes. In *New Perspectives on the Caledonides of Scandinavia and Related Areas* (eds F. Corfu, D. Gasser & D. Chew), pp. 131–55. Geological Society of London, Special Publication no. 390.

GEWEKE, J. F. & SINGLETON, K. J. 1980. Interpreting the likelihood ratio statistic in factor models when sample size is small. *Journal of the American Statistical Association* **75**, 133–7.

GEYER, G., ELICKI, O., FATKA, O. & ZYLINSKA, A. 2008. Cambrian. In *The Geology of Central Europe. Volume 1: Precambrian and Palaeozoic* (ed. T. McCann), pp. 155–202. London: The Geological Society.

GHIENNE, J.-F. 2003. Late Ordovician sedimentary environments, glacial cycles, and post-glacial transgression in the Taoudeni Basin, West Africa. *Palaeogeography, Palaeoclimatology, Palaeoecology* **189**, 117–45.

GHIENNE, J. F., MONOD, O., KOZLU, H. & DEAN, W. T. 2010. Cambrian–Ordovician depositional sequences in the Middle East: a perspective from Turkey. *Earth-Science Reviews* **101**, 101–46.

GIACOMINI, F., BOMPAROLA, R. M. & GHEZZO, C. 2005. Petrology and geochronology of metabasites with eclogite facies relics from NE Sardinia: constraints for the Palaeozoic evolution of Southern Europe. *Lithos* **82**, 221–48.

GIL IBARGUCHI, J. I., NAVIDAD, M. & ORTEGA, L. A. 1990. Ordovician and Silurian igneous rocks and orthogeneisses in the Catalonian Coastal Ranges. *Acta Geológica Hispánica* **25**, 23–9.

GOLONKA, J. & FORD, D. 2000. Pangean (Late Carboniferous-Middle Jurassic) paleoenvironment and lithofacies. *Palaeogeography, Palaeoclimatology, Palaeoecology* **161**, 1–34.

GUTIÉRREZ-MARCO, J. C., DE SAN JOSÉ, M. A. & PIEREN, A. P. L. 1990. Post-Cambrian Palaeozoic stratigraphy, Central Iberian Zone. In *Pre-Mesozoic Geology of Iberia* (ed. R. D. Dallmeyer), pp. 31–49. Berlin: Springer.

GUTIÉRREZ-MARCO, J. C., ROBARDET, M., RÁBANO, I., SARMIENTO, G. N., SAN JOSÉ LANCHA, M. A., HERRANZ, P. & PIEREN PIDAL, A. P. 2002. Ordovician. In *The Geology of Spain* (eds W. W. Gibbons & T. Moreno), pp. 31–49. London: Geological Society of London.

Halpin, J. A., Daczko, N. R., Milan, L. A. & Clarke, G. L. 2012. Decoding near-concordant U–Pb zircon ages spanning several hundred million years: recrystallisation, metamictisation or diffusion? *Contributions to Mineralogy and Petrology* **163**, 67–85.

Hammann, W. 1992. The Ordovician trilobites from the Iberian chains in the province of Aragon, NE-Spain. 1. The trilobites of the Cystoid Limestone (Ashgill series). *Beringeria* **6**, 1–219.

Handy, M. R., Ustaszewski, K. & Kissling, E. 2015. Reconstructing the Alps–Carpathians–Dinarides as a key to understanding switches in subduction polarity, slab gaps and surface motion. *International Journal of Earth Sciences* **104**, 1–26.

Hawkesworth, C., Cawood, P. & Dhuime, B. 2013. Continental growth and the crustal record. *Tectonophysics* **609**, 651–60.

Heinrichs, T., Siegesmund, S., Frei, D., Drobe, M. & Schulz, B. 2012. Provenance signatures from whole-rock geochemistry and detrital zircon ages of metasediments from the Austroalpine basement south of the Tauern window (eastern Tyrol, Austria). *GeoAlp* **9**, 156–85.

Henderson, B. J., Collins, W. J., Murphy, J. B., Gutierrez-Alonso, G. & Hand, M. 2016. Gondwanan basement terranes of the Variscan–Appalachian orogen: Baltican, Saharan and West African hafnium isotopic fingerprints in Avalonia, Iberia and the Armorican Terranes. *Tectonophysics* **681**, 278–304.

Hietpas, J., Samson, S., Moecher, D. & Chakraborty, S. 2011. Enhancing tectonic and provenance information from detrital zircon studies: assessing terrane-scale sampling and grain-scale characterization. *Journal of the Geological Society, London* **168**, 309–18.

Hofmann, M., Linnemann, U., Rai, V., Becker, S., Gärtner, A. & Sagawe, A. 2011. The India and South China cratons at the margin of Rodinia — synchronous Neoproterozoic magmatism revealed by LA-ICP-MS zircon analyses. *Lithos* **123**, 176–87.

Horbe, A. M. C., Motta, M. B., de Almeida, C. M., Dantas, E. L. & Vieira, L. C. 2013. Provenance of Pliocene and recent sedimentary deposits in western Amazônia, Brazil: consequences for the paleodrainage of the Solimões-Amazonas River. *Sedimentary Geology* **296**, 9–20.

Javier Álvaro, J., Colmenar, J., Monceret, E., Pouclet, A. & Vizcaïno, D. 2016. Late Ordovician (post-Sardic) rifting branches in the North Gondwanan Montagne Noire and Mouthoumet massifs of southern France. *Tectonophysics* **681**, 111–23.

Jimenez Millan, J. & Velilla, N. 1998. Mn-Fe spinels and silicates in manganese-rich rocks from the Ossa-Morena Zone, southern Iberian Massif, southwestern Spain. *The Canadian Mineralogist* **36**, 701–11.

Johnson, S. C. & McLeod, M. J., 1996. The New River Belt: a unique segment along the western margin of the Avalon composite terrane, southern New Brunswick, Canada. In *Avalonian and Related Peri-Gondwana Terranes of the Circum-North Atlantic* (eds R. D. Nance & M. D. Thompson), pp. 149–64. Geological Society of America Special Papers no. 304.

Julivert, M., Fontbote, J. M., Ribeiro, A. & Conde, L. N. 1972. *Mapa Tectónico de la Península Ibérica y Baleares*. Madrid: Instituto Geológico y Minero de España.

Kelly, N. M., Clarke, G. L. & Fanning, C. M. 2002. A two-stage evolution of the Neoproterozoic Rayner Structural Episode: new U–Pb sensitive high resolution ion microprobe constraints from the Oygarden Group, Kemp Land, East Antarctica. *Precambrian Research* **116**, 307–30.

Kelly, N. M., Clarke, G. L. & Fanning, C. M. 2004. Archaean crust in the Rayner Complex of east Antarctica: Oygarden Group of islands, Kemp Land. *Transactions of the Royal Society of Edinburgh: Earth Sciences* **95**, 491–510.

Kennan, P. S. & Morris, J. H. 1999. Manganiferous ironstones in the early Ordovician Manx Group, Isle of Man: a protolith of coticule? In *In Sight of the Suture: The Palaeozoic Geology of the Isle of Man in its Iapetus Ocean Context* (eds N. H. Woodcock, D. G. Quirk, W. R. Fitches & R. P. Barnes), pp. 109–19. Geological Society of London, Special Publication no. 160.

Keppie, J. D. & Krogh, T. E. 2000. 440 Ma igneous activity in the Meguma Terrane, Nova Scotia, Canada; part of the Appalachian overstep sequence? *American Journal of Science* **300**, 528–38.

Kolodner, K., Avigad, D., McWilliams, M., Wooden, J. L., Weissbrod, T. & Feinstein, S. 2006. Provenance of north Gondwana Cambrian–Ordovician sandstone: U–Pb SHRIMP dating of detrital zircons from Israel and Jordan. *Geological Magazine* **143**, 367–91.

Košler, J., Konopásek, J., Sláma, J. & Vrána, S. 2014. U–Pb zircon provenance of Moldanubian metasediments in the Bohemian Massif. *Journal of the Geological Society, London* **171**, 83–95.

Kossmat, F. 1927. Gliederung des varistischen Gebirgsbaues. *Abhandlungen des Sächsischen Geologischen Landesamts* **1**, 1–39.

Kramm, U. 1976. The coticule rocks (spessartine quartzites) of the Venn-Stavelot Massif, Ardennes, a volcanoclastic metasediment? *Contributions to Mineralogy and Petrology* **56**, 135–55.

Krawczyk, C. M., McCann, T., Cocks, L. R. M., England, R. W., McBride, J. H. & Wybraniez, S. 2008. Caledonian tectonics. In *The Geology of Central Europe. Volume 1: Precambrian and Palaeozoic* (ed. T. McCann), pp. 303–4381. London: The Geological Society.

Kreuzer, H., Seidel, E., Schüssler, U., Okrusch, M., Lenz, K.-L. & Raschka, H. 1989. K–Ar geochronology of different tectonic units at the northwestern margin of the Bohemian Massif. *Tectonophysics* **157**, 149–78.

Kroner, U., Hahn, T., Romer, R. L. & Linnemann, U. 2007. The Variscan orogeny in the Saxo-Thuringian zone—heterogenous overprint of Cadomian/Paleozoic Peri-Gondwana crust. In *The Evolution of the Rheic Ocean: From Avalonian–Cadomian Active Margin to Alleghenian–Variscan Collision* (eds U. Linnemann, R. D. Nance, P. Kraft & G. Zulauf), pp. 153–72. Geological Society of America, Special Papers no. 423.

Kroner, U. & Romer, R. L. 2010. The Saxo-Thuringian Zone–tip of the Armorican spur and part of the Gondwana plate. In *Pre-Mesozoic Geology of Saxo-Thuringia–From the Cadomian Active Margin to the Variscan Orogen* (eds U. Linnemann & R. L. Romer), pp. 371–94. Stuttgart: Schweizerbart.

Kroner, U. & Romer, R. L. 2013. Two plates – many subduction zones: the Variscan orogeny reconsidered. *Gondwana Research* **24**, 298–329.

Kroner, U., Roscher, M. & Romer, R. L. 2016. Ancient plate kinematics derived from the deformation pattern of continental crust: Paleo- and Neo-Tethys opening coeval with prolonged Gondwana–Laurussia convergence. *Tectonophysics* **681**, 220–33.

Kruskal, J. B. 1964. Multidimensional scaling by optimizing goodness of fit to a nonmetric hypothesis. *Psychometrika* **29**, 1–27.

Kruskal, J. B. & Wish, M. 1978. *Multidimensional Scaling*. Newbury Park: Sage Publications.

Kryza, R. & Fanning, C. M. 2007. Devonian deep-crustal metamorphism and exhumation in the Variscan Orogen: evidence from SHRIMP zircon ages from the HT-HP granulites and migmatites of the Góry Sowie (Polish Sudetes). *Geodinamica Acta* **20**, 159–75.

Küster, D., Romer, R. L., Tolessa, D., Zerihun, D., Bheemalingeswara, K., Melcher, F. & Oberthür, T. 2009. The Kenticha rare-element pegmatite, Ethiopia: internal differentiation, U–Pb age and Ta mineralization. *Mineralium Deposita* **44**, 723–50.

Langone, A., Braga, R., Massonne, H.-J. & Tiepolo, M. 2011. Preservation of old (prograde metamorphic) U–Th–Pb ages in unshielded monazite from the high-pressure paragneisses of the Variscan Ulten Zone (Italy). *Lithos* **127**, 68–85.

Lardeaux, J. M., Ledru, P., Daniel, I. & Duchene, S. 2001. The Variscan French Massif Central—a new addition to the ultra-high pressure metamorphic 'club': exhumation processes and geodynamic consequences. *Tectonophysics* **332**, 143–67.

Ledent, D., Patterson, C. & Tilton, G. R. 1964. Ages of zircon and feldspar concentrates from North American beach and river sands. *The Journal of Geology* **72**, 112–22.

Le Heron, D. P., Ghienne, J.-F., El Houicha, M., Khoukhi, Y. & Rubino, J.-L. 2007. Maximum extent of ice sheets in Morocco during the Late Ordovician glaciation. *Palaeogeography, Palaeoclimatology, Palaeoecology* **245**, 200–26.

Linan, E., Gozalo, R., Palacios, T., Vintaned, J. A. G., Ugidos, J. M. & Mayoral, E. 2002. Cambrian. In *The Geology of Spain* (eds W. Gibbons & T. Moreno), pp. 17–30. London: Geological Society of London.

Linnemann, U., D'Lemos, R., Drost, K., Jeffries, T., Gerdes, A., Romer, R. L., Samson, S. D. & Strachan, R. A. 2008a. Cadomian tectonics. In *The Geology of Central Europe. Volume 1: Precambrian and Palaeozoic* (ed. T. McCann), pp. 103–54. London: The Geological Society.

Linnemann, U., Gehmlich, M., Tichomirowa, M., Buschmann, B., Nasdala, L., Jonas, P., Lützner, H. & Bombach, K. 2000. From Cadomian subduction to Early Palaeozoic rifting: the evolution of Saxo-Thuringia at the margin of Gondwana in the light of single zircon geochronology and basin development (Central European Variscides, Germany). In *Orogenic Processes: Quantification and Modelling in the Variscan Belt* (eds. W. Franke, R. Altherr, V. Haak, O. Ocncken & D. Tanner), pp. 131–53. Geological Society of London: Special Publication no. 179.

Linnemann, U., Gerdes, A., Hofmann, M. & Marko, L. 2014. The Cadomian Orogen: Neoproterozoic to Early Cambrian crustal growth and orogenic zoning along the periphery of the West African Craton—constraints from U–Pb zircon ages and Hf isotopes (Schwarzburg Antiform, Germany). *Precambrian Research* **244**, 236–78.

Linnemann, U., Herbosch, A., Liégeois, J.-P., Pin, C., Gärtner, A. & Hofmann, M. 2012. The Cambrian to Devonian odyssey of the Brabant Massif within Avalonia: a review with new zircon ages, geochemistry, Sm–Nd isotopes, stratigraphy and palaeogeography. *Earth-Science Reviews* **112**, 126–54.

Linnemann, U. & Heuse, T. 2000. The Ordovician of the Schwarzburg Anticline: geotectonic setting, biostratigraphy and sequence stratigraphy (Saxo-Thuringian Terrane, Germany). *Zeitschrift der deutschen Geologischen Gesellschaft* **151**, 471–91.

Linnemann, U., Hofmann, M., Romer, R. L. & Gerdes, A. 2010a. Transitional stages between the Cadomian and Variscan orogenies: basin development and tectono-magmatic evolution of the southern margin of the Rheic Ocean in the Saxo-Thuringian Zone (North Gondwana shelf). In *Pre-Mesozoic Geology of Saxo-Thuringia — from the Cadomian Active Margin to the Variscan Orogen* (ed. U. Linnemann & R. L. Romer), pp. 59–98. Stuttgart: Schweizerbart.

Linnemann, U., McNaughton, N. J., Romer, R. L., Gehmlich, M., Drost, K. & Tonk, C. 2004. West African provenance for Saxo-Thuringia (Bohemian Massif): did Armorica ever leave pre-Pangean Gondwana? – U/Pb-SHRIMP zircon evidence and the Nd-isotopic record. *International Journal of Earth Sciences* **93**, 683–705.

Linnemann, U., Ouzegane, K., Drareni, A., Hofmann, M., Becker, S., Gärtner, A. & Sagawe, A. 2011. Sands of West Gondwana: an archive of secular magmatism and plate interactions—a case study from the Cambro-Ordovician section of the Tassili Ouan Ahaggar (Algerian Sahara) using U–Pb–LA-ICP-MS detrital zircon ages. *Lithos* **123**, 188–203.

Linnemann, U., Pereira, F., Jeffries, T. E., Drost, K. & Gerdes, A. 2008b. The Cadomian Orogeny and the opening of the Rheic Ocean: the diacrony of geotectonic processes constrained by LA-ICP-MS U–Pb zircon dating (Ossa-Morena and Saxo-Thuringian Zones, Iberian and Bohemian Massifs). *Tectonophysics* **461**, 21–43.

Linnemann, U., Romer, R. L., Gerdes, A., Jeffries, T. E., Drost, K. & Ulrich, J. 2010b. The Cadomian orogeny in the Saxo-Thuringian zone. In *Pre-Mesozoic Geology of Saxo-Thuringia–From the Cadomian Active Margin to the Variscan Orogen* (eds U. Linneman & R. L. Romer), pp. 37–58. Stuttgart: Schweizerbart.

Lotze, F. 1945. Zur Gliederung der Varisziden in der Iberischen Meseta. *Geotektonische Forschungen* **6**.

Lotze, F. 1956. Das Präkambrium Spaniens. *Neues Jahrbuch für Geologie und Paläontologie, Monatschefte* **8**, 373–80.

Lucks, H., Schulz, B., Audren, C. & Triboulet, C. 2002. Variscan pressure-temperature evolution of garnet pyroxenites and amphibolites in the Baie d'Audierne metamorphic series, Brittany (France). In *Variscan–Appalachian Dynamics: The Building of the Late Paleozoic Basement* (eds J. R. M. Catalán, J. R. D. Hatcher, R. Arenas & F. D. García), pp. 89–103. Geological Society of America, Special Papers no. 364.

MacDonald, L. A., Barr, S. M., White, C. E. & Ketchum, J. W. F. 2002. Petrology, age, and tectonic setting of the White Rock Formation, Meguma terrane, Nova Scotia: evidence for Silurian continental rifting. *Canadian Journal of Earth Sciences* **39**, 259–77.

Martínez Catalán, J. R. 2012. The Central Iberian arc, an orocline centered in the Iberian Massif and some implications for the Variscan belt. *International Journal of Earth Sciences* **101**, 1299–314.

Martínez Catalán, J. R., Rubio Pascual, F. J., Montes, A. D., Fernández, R. D., Barreiro, J. G., Dias Da Silva, Í., Clavijo, E. G., Ayarza, P. & Alcock, J. E. 2014. The late Variscan HT/LP metamorphic event in NW and Central Iberia: relationships to crustal thickening, extension, orocline development and crustal evolution. In *Geomechanics and Geology* (eds. J. P. Turner, D. Healy, R. R. Hillis & M. J. Welch), pp. 225–47. Geological Society of London, Special Publication no. 405.

Matte, P. 1986. Tectonics and plate tectonics model for the Variscan belt of Europe. *Tectonophysics* **126**, 329–74.

Matte, P. 2001. The Variscan collage and orogeny (480–290 Ma) and the tectonic definition of the Armorica microplate: a review. *Terra Nova* **13**, 122–8.

Matteini, M., Dantas, E. L., Pimentel, M. M., de Alvarenga, C. J. S. & Dardenne, M. A. 2012. U–Pb and Hf isotope study on detrital zircons from the Paranoá Group, Brasília Belt Brazil: constraints on depositional age at Mesoproterozoic – Neoproterozoic transition and tectono-magmatic events in the São Francisco craton. *Precambrian Research* **206–207**, 168–81.

Mattinson, J. M. 1987. U–Pb ages of zircons: a basic examination of error propagation. *Chemical Geology: Isotope Geoscience Section* **66**, 151–62.

Mazur, S., Szczepański, J., Turniak, K. & McNaughton, N. J. 2012. Location of the Rheic suture in the eastern Bohemian Massif: evidence from detrital zircon data. *Terra Nova* **24**, 199–206.

McLennan, S. M., Hemming, S., McDaniel, D. K. & Hanson, G. N. 1993. Geochemical approaches to sedimentation, provenance, and tectonics. In *Processes Controlling the Composition of Clastic Sediments* (eds M. J. Johnsson & A. Basu), pp. 21–40. Geological Society of America, Special Papers no. 284.

Meinhold, G., Kostopoulos, D., Frei, D., Himmerkus, F. & Reischmann, T. 2010. U–Pb LA-SF-ICP-MS zircon geochronology of the Serbo-Macedonian Massif, Greece: palaeotectonic constraints for Gondwana-derived terranes in the Eastern Mediterranean. *International Journal of Earth Sciences* **99**, 813–32.

Meinhold, G., Morton, A. C. & Avigad, D. 2013. New insights into peri-Gondwana paleogeography and the Gondwana super-fan system from detrital zircon U–Pb ages. *Gondwana Research* **23**, 661–5.

Meinhold, G., Morton, A. C., Fanning, C. M., Frei, D., Howard, J. P., Phillips, R. J., Strogen, D. & Whitham, A. G. 2011. Evidence from detrital zircons for recycling of Mesoproterozoic and Neoproterozoic crust recorded in Paleozoic and Mesozoic sandstones of southern Libya. *Earth and Planetary Science Letters* **312**, 164–75.

Mélou, M., Oulebsir, L. & Paris, F. 1999. Brachiopodes et chitinozoaires ordoviciens dans le NE du Sahara algérien: implications stratigraphiques et paléógéographiques. *Geobios* **32**, 822–39.

Mikhalsky, E. V., Beliatsky, B. V., Sheraton, J. W. & Roland, N. W. 2006. Two distinct Precambrian terranes in the Southern Prince Charles Mountains, East Antarctica: SHRIMP dating and geochemical constraints. *Gondwana Research* **9**, 291–309.

Moecher, D. P. & Samson, S. D. 2006. Differential zircon fertility of source terranes and natural bias in the detrital zircon record: implications for sedimentary provenance analysis. *Earth and Planetary Science Letters* **247**, 252–66.

Moghadam, H. S., Li, X.-H., Griffin, W. L., Stern, R. J., Thomsen, T. B., Meinhold, G., Aharipour, R. & O'Reilly, S. Y. 2017. Early Paleozoic tectonic reconstruction of Iran: tales from detrital zircon geochronology. *Lithos* **268–271**, 87–101.

Molzahn, M., Anthes, G. & Reischmann, T. 1998. Single zircon Pb/Pb age geochronology and isotope systematics of the Rhenohercynian basement. *Terra Nostra* **98**, 67–8.

Monod, O., Kozlu, H., Ghienne, J. F., Dean, W. T., Günay, Y., Hérissé, A. L., Paris, F. & Robardet, M. 2003. Late Ordovician glaciation in southern Turkey. *Terra Nova* **15**, 249–57.

Morton, A. C. & Hallsworth, C. 1994. Identifying provenance-specific features of detrital heavy mineral assemblages in sandstones. *Sedimentary Geology* **90**, 241–56.

Moryc, W. & Łydka, K. 2012. Sedimentation and tectonics of the Upper Proterozoic-Lower Cambrian deposits of the southern Małopolska Massif (SE Poland). *Geological Quarterly* **44**, 12–47.

Murphy, J. B., Fernández-Suárez, J., Keppie, J. D. & Jeffries, T. E. 2004a. Contiguous rather than discrete Paleozoic histories for the Avalon and Meguma terranes based on detrital zircon data. *Geology* **32**, 585–8.

Murphy, J. B., Pisarevsky, S. A., Nance, R. D. & Keppie, J. D. 2004b. Neoproterozoic—Early Paleozoic evolution of peri-Gondwanan terranes: implications for Laurentia-Gondwana connections. *International Journal of Earth Sciences* **93**, 659–82.

Murphy, J. B., Strachan, R. A., Nance, R. D., Parker, K. D. & Fowler, M. B. 2000. Proto-Avalonia: a 1.2–1.0 Ga tectonothermal event and constraints for the evolution of Rodinia. *Geology* **28**, 1071–4.

Nägler, T. F., Schafer, H.-J. & Gebauer, D. 1995. Evolution of the Western European continental crust: implications from Nd and Pb isotopes in Iberian sediments. *Chemical Geology* **121**, 345–57.

Nance, R. D., Gutiérrez-Alonso, G., Keppie, J. D., Linnemann, U., Murphy, J. B., Quesada, C., Strachan, R. A. & Woodcock, N. H. 2010. Evolution of the Rheic Ocean. *Gondwana Research* **17**, 194–222.

Nance, R. D. & Linnemann, U. 2008. The Rheic Ocean: origin, evolution, and significance. *GSA Today* **18**, 4–12.

Nie, J., Peng, W., Möller, A., Song, Y., Stockli, D. F., Stevens, T., Horton, B. K., Liu, S., Bird, A., Oalmann, J., Gong, H. & Fang, X. 2014. Provenance of the upper Miocene–Pliocene Red Clay deposits of the Chinese loess plateau. *Earth and Planetary Science Letters* **407**, 35–47.

Noblet, C. & Lefort, J. P. 1990. Sedimentological evidence for a limited separation between Armorica and Gondwana during the Early Ordovician. *Geology* **18**, 303–6.

Nutman, A. P., Green, D. H., Cook, C. A., Styles, M. T. & Holdsworth, R. E. 2001. SHRIMP U–Pb zircon dating of the exhumation of the Lizard Peridotite and its emplacement over crustal rocks: constraints for tectonic models. *Journal of the Geological Society, London* **158**, 809–20.

O'Brien, S. J., Wardle, R. J. & King, A. F. 1983. The Avalon Zone: a Pan-African terrane in the Appalachian Orogen of Canada. *Geological Journal* **18**, 195–222.

Oczlon, M. S., Seghedi, A. & Carrigan, C. W. 2007. Avalonian and Baltican terranes in the Moesian Platform (southern Europe, Romania, and Bulgaria) in the context of Caledonian terranes along the southwestern margin of the East European craton. In *The Evolution of the Rheic Ocean: From Avalonian-Cadomian Active Margin to Alleghenian-Variscan Collision* (eds U. Linneman, R. D. Nance, P. Kraft & G. Zulauf), pp. 375–400. Geological Society of America, Special Papers no. 423.

Ordóñez Casado, B., Gebauer, D., Schäfer, H. J., Gil Ibarguchi, J. I. & Peucat, J. J. 2001. A single Devonian subduction event for the HP/HT metamorphism of the Cabo Ortegal complex within the Iberian Massif. *Tectonophysics* **332**, 359–85.

Orejana, D., Merino Martínez, E., Villaseca, C. & Andersen, T. 2015. Ediacaran–Cambrian paleogeography and geodynamic setting of the Central Iberian Zone: constraints from coupled U–Pb–Hf isotopes of detrital zircons. *Precambrian Research* **261**, 234–51.

Paris, F. & Robardet, M. 1990. Early Palaeozoic palaeobiogeography of the Variscan regions. *Tectonophysics* **177**, 193–213.

Pereira, M. F. 2015. Potential sources of Ediacaran strata of Iberia: a review. *Geodinamica Acta* **27**, 1–14.

Pereira, M. F., Chichorro, M., Linnemann, U., Eguiluz, L. & Silva, J. B. 2006. Inherited arc signature in Ediacaran and Early Cambrian basins of the Ossa-Morena Zone (Iberian Massif, Portugal): paleogeographic link with European and North African Cadomian correlatives. *Precambrian Research* **144**, 297–315.

Pérez-Cáceres, I., Martínez Poyatos, D., Simancas, J. F. & Azor, A. 2017. Testing the Avalonian affinity of the South Portuguese Zone and the Neoproterozoic evolution of SW Iberia through detrital zircon populations. *Gondwana Research* **42**, 177–92.

Perroud, H. & Bonhommet, N. 1984. A Devonian palaeomagnetic pole for Armorica. *Geophysical Journal of the Royal Astronomical Society* **77**, 839–45.

Perroud, H., Calza, F. & Khattach, D. 1991. Paleomagnetism of the Silurian volcanism at Almaden, southern Spain. *Journal of Geophysical Research: Solid Earth* **96**, 1949–62.

Pettersson, C. H., Pease, V. & Frei, D. 2010. Detrital zircon U–Pb ages of Silurian–Devonian sediments from NW Svalbard: a fragment of Avalonia and Laurentia? *Journal of the Geological Society, London* **167**, 1019–32.

Pharaoh, T. C. 1999. Palaeozoic terranes and their lithospheric boundaries within the Trans-European Suture Zone (TESZ): a review. *Tectonophysics* **314**, 17–41.

Pharaoh, T. C. & Carney, J. N. 2000. Introduction. In *Precambrian Rocks of England and Wales* (eds J. Carney, J. M. Horak, T. C. Pharao, W. Gibbons, D. Wilson, W. J. Barclay, R. E. Bevins, J. C. W. Cope & T. D. Ford), pp. 1–18. Geological Conservation Review Series no. 20.

Pique, A. & Michard, A. 1989. Moroccan Hercynides; a synopsis; the Paleozoic sedimentary and tectonic evolution at the northern margin of West Africa. *American Journal of Science* **289**, 286–330.

Poli, M. E. & Zanferrari, A. 1992. The Agordo basement (NE Italy): a 500 Ma-long geological record in the Southalpine crust. In *Contribution to the Geology of Italy with Special Regard to the Paleozoic Basements: A Volume Dedicated to Tommaso Cocozza* (eds L. Carmignani & F. P. Sassi), pp. 283–96. IGCP Project 276, Newsletter no. 5.

Pollock, J. C., Hibbard, J. P. & van Staal, C. R. 2011. A paleogeographical review of the peri-Gondwanan realm of the Appalachian orogen. *Canadian Journal of Earth Sciences* **49**, 259–88.

Pullen, A., Ibáñez-Mejía, M., Gehrels, G. E., Ibáñez-Mejía, J. C. & Pecha, M. 2014. What happens when n = 1000? Creating large-n geochronological datasets with LA-ICP-MS for geologic investigations. *Journal of Analytical Atomic Spectrometry* **29**, 971–80.

Razali, N. M. & Wah, Y. B. 2011. Power comparisons of Shapiro-Wilk, Kolmogorov-Smirnov, *Lilliefors and Anderson-Darling tests Journal of Statistical Modeling and Analytics* **2**, 21–33.

Rittner, M., Vermeesch, P., Carter, A., Bird, A., Stevens, T., Garzanti, E., Andò, S., Vezzoli, G., Dutt, R., Xu, Z. & Lu, H. 2016. The provenance of Taklamakan desert sand. *Earth and Planetary Science Letters* **437**, 127–37.

Robardet, M. 2002. Alternative approach to the Variscan Belt in southwestern Europe: preorogenic paleobiogeographical constraints. In *Variscan–Appalachian Dynamics: The Building of the Late Paleozoic Basement* (eds J. R. M. Catalán, J. R. D. Hatcher, R. Arenas & F. D. García), pp. 1–15. Geological Society of America, Special Papers no. 364.

Robardet, M. & Doré, F. 1988. The late Ordovician diamictic formations from southwestern Europe: North-Gondwana glaciomarine deposits. *Palaeogeography, Palaeoclimatology, Palaeoecology* **66**, 19–31.

Robardet, M. & Gutiérrez-Marco, J. C. 2002. Silurian. In *The Geology of Spain* (eds W. W. Gibbons & T. Moreno), pp. 51–66. London: Geological Society of London.

Robardet, M., Verniers, J., Feist, R. & Paris, F. 1994. The pre-Variscan Palaeozoic successions in France, palaeogeographic and geodynamic setting. *Geologie de la France* **3**, 3–31.

Rogers, N., van Staal, C. R., McNicoll, V., Pollock, J., Zagorevski, A. & Whalen, J. 2006. Neoproterozoic and Cambrian arc magmatism along the eastern margin of the Victoria Lake Supergroup: a remnant of Ganderian basement in central Newfoundland? *Precambrian Research* **147**, 320–41.

Rolet, J., Gresselin, F., Jegouzo, P., Ledru, P. & Wyns, R. 1994. Intracontinental Hercynian Events in the Armorican Massif. In *Pre-Mesozoic Geology in France and Related Areas* (eds J. Chantraine, J. Rolet, D. S. Santallier, A. Piqué & J. D. Keppie), pp. 195–219. Berlin, Heidelberg: Springer.

Romer, R. L. & Hahne, K. 2010. Life of the Rheic Ocean: scrolling through the shale record. *Gondwana Research* **17**, 236–53.

Romer, R. L., Kirsch, M. & Kroner, U. 2011. Geochemical signature of Ordovician Mn-rich sedimentary rocks on the Avalonian shelf. *Canadian Journal of Earth Sciences* **48**, 703–18.

Romer, R. L. & Kroner, U. 2015. Sediment and weathering control on the distribution of Paleozoic magmatic tin–tungsten mineralization. *Mineralium Deposita* **50**, 327–38.

Romer, R. L. & Kroner, U. 2016. Phanerozoic tin and tungsten mineralization – tectonic controls on the distribution of enriched protoliths and heat sources for crustal melting. *Gondwana Research* **31**, 60–95.

Rösel, D., Boger, S. D., Möller, A., Gaitzsch, B., Barth, M., Oalmann, J. & Zack, T. 2014. Indo-Antarctic derived detritus on the northern margin of Gondwana: evidence for continental-scale sediment transport. *Terra Nova* **26**, 64–71.

Rossi, P., Oggiano, G. & Cocherie, A. 2009. A restored section of the “southern Variscan realm” across the Corsica–Sardinia microcontinent. *Comptes Rendus Geoscience* **341**, 224–38.

Rousseeuw, P. J. 1987. Silhouettes: a graphical aid to the interpretation and validation of cluster analysis. *Journal of Computational and Applied Mathematics* **20**, 53–65.

Rubatto, D., Ferrando, S., Compagnoni, R. & Lombardo, B. 2010. Carboniferous high-pressure metamorphism of Ordovician protoliths in the Argentera Massif (Italy), southern European Variscan belt. *Lithos* **116**, 65–76.

Satkoski, A. M., Barr, S. M. & Samson, S. D. 2010. Provenance of Late Neoproterozoic and Cambrian sediments in Avalonia: constraints from detrital zircon ages and Sm–Nd isotopic compositions in Southern New Brunswick, Canada. *The Journal of Geology* **118**, 187–200.

Schaltegger, U., Schneider, J.-L., Maurin, J.-C. & Corfu, F. 1996. Precise UPb chronometry of 345–340 Ma old magmatism related to syn-convergence extension in the Southern Vosges (Central Variscan Belt). *Earth and Planetary Science Letters* **144**, 403–19.

Schmid, S. M., Fügenschuh, B., Kissling, E. & Schuster, R. 2004. Tectonic map and overall architecture of the Alpine orogen. *Eclogae Geologicae Helvetiae* **97**, 93–117.

Schulz, K. J., Stewart, D. B., Tucker, R. D., Pollock, J. C. & Ayuso, R. A. 2008. The Ellsworth terrane, coastal Maine: geochronology, geochemistry, and Nd–Pb isotopic composition—implications for the rifting of Ganderia. *Geological Society of America Bulletin* **120**, 1134–58.

Scotese, C. R., Boucot, A. J. & McKerrow, W. S. 1999. Gondwanan palaeogeography and palaeoclimatology. *Journal of African Earth Sciences* **28**, 99–114.

Servais, T., Dzik, J., Fatka, O., Heuse, T., Vecoli, M. & Verniers, J. 2008. Ordovician. In *The Geology of Central Europe. Volume 1: Precambrian and Palaeozoic* (ed. T. McCann), pp. 203–48. London: The Geological Society.

Sharland, P. R., Archer, R., Casey, D. M., Davies, R. B., Hall, S. H., Heward, A. P., Horbury, A. D. & Simmons, M. D. 2001. *The Chrono-sequence Stratigraphy of the Arabian Plate*. GeoArabia Special Publication no. 2.

Sharman, G. R. & Johnstone, S. A. 2017. Sediment unmixing using detrital geochronology. *Earth and Planetary Science Letters* **477**, 183–94.

Shaw, J., Gutiérrez-Alonso, G., Johnston, S. T. & Pastor Galán, D. 2014. Provenance variability along the Early Ordovician north Gondwana margin: paleogeographic and tectonic implications of U–Pb detrital zircon ages from the Armorican Quartzite of the Iberian Variscan belt. *Geological Society of America Bulletin* **126**, 702–19.

Shu, L. S., Deng, X. L., Zhu, W. B., Ma, D. S. & Xiao, W. J. 2011. Precambrian tectonic evolution of the Tarim Block, NW China: new geochronological insights from the Quruqtagh domain. *Journal of Asian Earth Sciences* **42**, 774–90.

Sircombe, K. N. 2000. Quantitative comparison of large sets of geochronological data using multivariate analysis: a provenance study example from Australia. *Geochimica et Cosmochimica Acta* **64**, 1593–616.

Slama, J. 2016. Rare late Neoproterozoic detritus in SW Scandinavia as a response to distant tectonic processes. *Terra Nova* **28**, 394–401.

Sláma, J. & Košler, J. 2012. Effects of sampling and mineral separation on accuracy of detrital zircon studies. *Geochemistry, Geophysics, Geosystems* **13**.

Squire, R. J., Campbell, I. H., Allen, C. M. & Wilson, C. J. L. 2006. Did the Transgondwanan Supermountain trigger the explosive radiation of animals on Earth? *Earth and Planetary Science Letters* **250**, 116–33.

Stampfli, G. M. & Borel, G. D. 2002. A plate tectonic model for the Paleozoic and Mesozoic constrained by dynamic plate boundaries and restored synthetic oceanic isochrons. *Earth and Planetary Science Letters* **196**, 17–33.

Stampfli, G. M., Hochard, C., Vérard, C., Wilhem, C. & von Raumer, J. 2013. The formation of Pangea. *Tectonophysics* **593**, 1–19.

Stampfli, G. M., von Raumer, J. F. & Borel, G. D. 2002. Paleozoic evolution of pre-Variscan terranes: from Gondwana to the Variscan collision. In *Variscan–Appalachian Dynamics: The Building of the Late Paleozoic Basement* (eds J. R. M. Catalán, J. R. D. Hatcher, R. Arenas & F. D. García), pp. 263–80. Geological Society of America, Special Papers no. 364.

Stephan, T., Kroner, U., Hahn, T., Hallas, P. & Heuse, T. 2016. Fold/cleavage relationships as indicator for late Variscan sinistral transpression at the Rheno-Hercynian–Saxo-Thuringian boundary zone, Central European Variscides. *Tectonophysics* **681**, 250–62.

Stevens, T., Carter, A., Watson, T. P., Vermeesch, P., Andò, S., Bird, A. F., Lu, H., Garzanti, E., Cottam, M. A. & Sevastjanova, I. 2013. Genetic linkage between the Yellow River, the Mu Us desert and the Chinese Loess Plateau. *Quaternary Science Reviews* **78**, 355–68.

Strachan, R. A. 2012. Late Neoproterozoic to Cambrian accretionary history of eastern Avalonia and Armorica on the Active Margin of Gondwana. In *Geological History of Britain and Ireland* (eds N. H. Woodcock & R. A. Strachan), pp. 133–49. Chichester: John Wiley & Sons, Ltd.

Strachan, R. A., Collins, A. S., Buchan, C., Nance, R. D., Murphy, J. B. & D'Lemos, R. S. 2007. Terrane analysis along a Neoproterozoic active margin of Gondwana: insights from U–Pb zircon geochronology. *Journal of the Geological Society, London* **164**, 57–60.

Strachan, R. A., Linnemann, U., Jeffries, T., Drost, K. & Ulrich, J. 2014. Armorican provenance for the mélange deposits below the Lizard ophiolite (Cornwall, UK): evidence for Devonian obduction of Cadomian and Lower Palaeozoic crust onto the southern margin of Avalonia. *International Journal of Earth Sciences* **103**, 1359–83.

Tait, J. A., Bachtadse, V., Franke, W. & Soffel, H. C. 1997. Geodynamic evolution of the European Variscan fold belt: palaeomagnetic and geological constraints. *Geologische Rundschau* **86**, 585–98.

Talavera, C., Montero, P., Martínez Poyatos, D. & Williams, I. S. 2012. Ediacaran to Lower Ordovician age for rocks ascribed to the Schist–Graywacke Complex (Iberian Massif, Spain): evidence from detrital zircon SHRIMP U–Pb geochronology. *Gondwana Research* **22**, 928–42.

Tatsumoto, M. & Patterson, C. 1964. Age studies of zircon and feldspar concentrates from the Franconia Sandstone. *The Journal of Geology* **72**, 232–42.

Tibshirani, R., Walther, G. & Hastie, T. 2001. Estimating the number of clusters in a data set via the gap statistic. *Journal of the Royal Statistical Society: Series B (Statistical Methodology)* **63**, 411–23.

Torsvik, T. H. & Cocks, L. R. M. 2013. Gondwana from top to base in space and time. *Gondwana Research* **24**, 999–1030.

Torsvik, T. H. & Rehnström, E. F. 2003. The Tornquist Sea and Baltica–Avalonia docking. *Tectonophysics* **362**, 67–82.

Torsvik, T. H., Smethurst, M. A., Meert, J. G., Van Der Voo, R., McKerrow, W. S., Brasier, M. D., Sturt, B. A. & Walderhaug, H. J. 1996. Continental break-up and collision in the Neoproterozoic and Palaeozoic – a tale of Baltica and Laurentia. *Earth-Science Reviews* **40**, 229–58.

Trombetta, A., Cirrincione, R., Corfu, F., Mazzoleni, P. & Pezzino, A. 2004. Mid-Ordovician U–Pb ages of porphyroids in the Peloritan Mountains (NE Sicily): palaeogeographical implications for the evolution of the Alboran microplate. *Journal of the Geological Society, London* **161**, 265–76.
Ugidos, J. M., Sánchez-Santos, J. M., Barba, P. & Valladares, M. I. 2010. Upper Neoproterozoic series in the Central Iberian, Cantabrian and West Asturian Leonese Zones (Spain): geochemical data and statistical results as evidence for a shared homogenised source area. *Precambrian Research* **178**, 51–8.
Ustaömer, P. A., Ustaömer, T., Gerdes, A. & Zulauf, G. 2011. Detrital zircon ages from a Lower Ordovician quartzite of the İstanbul exotic terrane (NW Turkey): evidence for Amazonian affinity. *International Journal of Earth Sciences* **100**, 23–41.
Valverde-Vaquero, P. & Dunning, G. R. 2000. New U–Pb ages for Early Ordovician magmatism in Central Spain. *Journal of the Geological Society, London* **157**, 15–26.
Van der Voo, R. 1988. Paleozoic paleogeography of North America, Gondwana, and intervening displaced terranes: comparisons of paleomagnetism with paleoclimatology and biogeographical patterns. *Geological Society of America Bulletin* **100**, 311–24.
Van Staal, C. R., Dewey, J. F., Niocaill, C. M. & McKerrow, W. S. 1998. The Cambrian–Silurian tectonic evolution of the northern Appalachians and British Caledonides: history of a complex, west and southwest Pacific-type segment of Iapetus. In *Lyell: The Past is the Key to the Present* (eds D. J. Blundell & A. C. Scott), pp. 197–242. Geological Society of London, Special Publication no. 143.
Veevers, J. J. 2004. Gondwanaland from 650–500 Ma assembly through 320 Ma merger in Pangea to 185–100 Ma breakup: supercontinental tectonics via stratigraphy and radiometric dating. *Earth-Science Reviews* **68**, 1–132.
Vermeesch, P. 2004. How many grains are needed for a provenance study? *Earth and Planetary Science Letters* **224**, 441–51.
Vermeesch, P. 2013. Multi-sample comparison of detrital age distributions. *Chemical Geology* **341**, 140–6.
Vermeesch, P., Resentini, A. & Garzanti, E. 2016. An R package for statistical provenance analysis. *Sedimentary Geology* **336**, 14–25.
Verniers, J., Maletz, J., Kříž, J., Žigaitė, Z., Paris, F., Schönlaub, H. P. & Wrona, R. 2008. *Silurian*. In *The Geology of Central Europe. Volume 1: Precambrian and Palaeozoic* (ed. T. McCann), pp. 249–302. London: The Geological Society.
Verniers, J., Pharaoh, T., André, L., Debacker, T. N., De Vos, W., Everaerts, M., Herbosch, A., Samuelsson, J., Sintubin, M. & Vecoli, M. 2002. The Cambrian to mid Devonian basin development and deformation history of Eastern Avalonia, east of the Midlands Microcraton: new data and a review. In *Palaeozoic Amalgamation of Central Europe* (eds J. A. Winchester, T. C. Pharao & J. Verniers), pp. 47–93. Geological Society of London, Special Publication no. 201.
Villas, E., Vennin, E., Álvaro, J. J., Hammann, W., Herrera, Z. A. & Piovano, E. L. 2002. The late Ordovician carbonate sedimentation as a major triggering factor of the Hirnantian glaciation. *Bulletin de la Societe geologique de France* **173**, 569–78.
von Raumer, J. F., Stampfli, G. M. & Bussy, F. 2003. Gondwana-derived microcontinents — the constituents of the Variscan and Alpine collisional orogens. *Tectonophysics* **365**, 7–22.
Vorster, C., Kramers, J. A. N., Beukes, N. I. C. & Van Niekerk, H. 2015. Detrital zircon U–Pb ages of the Palaeozoic Natal Group and Msikaba Formation, Kwazulu-Natal, South Africa: provenance areas in context of Gondwana. *Geological Magazine* **153**, 460–86.
Waldron, J. W. F., Schofield, D. I., White, C. E. & Barr, S. M. 2011. Cambrian successions of the Meguma Terrane, Nova Scotia, and Harlech Dome, North Wales: dispersed fragments of a peri-Gondwanan basin? *Journal of the Geological Society, London* **168**, 83–98.
Waldron, J. W. F., White, C. E., Barr, S. M., Simonetti, A. & Heaman, L. M. 2009. Provenance of the Meguma terrane, Nova Scotia: rifted margin of early Paleozoic Gondwana. *Canadian Journal of Earth Sciences* **46**, 1–8.
White, C. E., Barr, S. M., Bevier, M. L. & Kamo, S. 1994. A revised interpretation of Cambrian and Ordovician rocks in the Bourinot belt of central Cape Breton Island, Nova Scotia. *Atlantic Geology* **30**, 123–42.
Williams, S. H. 1993. *More Ordovician and Silurian Graptolites from the Exploits Subzone*. Newfoundland Department of Mines and Energy, Geological Survey Branch, Report 93-1, pp. 311–15.
Willner, A. P., Barr, S. M., Gerdes, A., Massonne, H.-J. & White, C. E. 2013. Origin and evolution of Avalonia: evidence from U–Pb and Lu–Hf isotopes in zircon from the Mira terrane, Canada, and the Stavelot–Venn Massif, Belgium. *Journal of the Geological Society, London* **170**, 769–84.
Yao, J., Shu, L., Santosh, M. & Li, J. 2012. Precambrian crustal evolution of the South China Block and its relation to supercontinent history: constraints from U–Pb ages, Lu–Hf isotopes and REE geochemistry of zircons from sandstones and granodiorite. *Precambrian Research* **208–211**, 19–48.
Young, T. P. 1990. Ordovician sedimentary facies and faunas of southwest Europe: palaeogeographic and tectonic implications. In *Palaeozoic Palaeogeography and Biogeography* (eds W. S. McKerrow & C. R. Scotese), pp. 421–30. Geological Society of London, Memoirs no. 12.
Zagorevski, A., Van Staal, C. R., Rogers, N., McNicoll, V. J. & Pollock, J. 2010. Middle Cambrian to Ordovician arc-backarc development on the leading edge of Ganderia, Newfoundland Appalachians. In *From Rodinia to Pangea: The Lithotectonic Record of the Appalachian Region* (eds R. P. Tollo, M. J. Bartholomew, J. P. Hibbard & P. M. Karabinos), pp. 367–96. Geological Society of America, Memoirs no. 206.
Žák, J. & Sláma, J. 2017. How far did the Cadomian ‘terranes’ travel from Gondwana during early Palaeozoic? A critical reappraisal based on detrital zircon geochronology. *International Geology Review*, published online 5 June 2017. doi: 10.1080/00206814.2017.1334599. 20 pp.
Zeh, A. & Gerdes, A. 2010. Baltica- and Gondwana-derived sediments in the Mid-German Crystalline Rise (Central Europe): implications for the closure of the Rheic ocean. *Gondwana Research* **17**, 254–63.
Zimmermann, U., Andersen, T., Madland, M. V. & Larsen, I. S. 2015. The role of U–Pb ages of detrital zircons in sedimentology – an alarming case study for the impact of sampling for provenance interpretation. *Sedimentary Geology* **320**, 38–50.

Zlatkin, O., Avigad, D. & Gerdes, A. 2014. Peri-Amazonian provenance of the Proto-Pelagonian basement (Greece), from zircon U–Pb geochronology and Lu–Hf isotopic geochemistry. *Lithos* **184–187**, 379–92.

Zlatkin, O., Avigad, D. & Gerdes, A. 2017. The Pelagonian terrane of Greece in the peri-Gondwanan mosaic of the Eastern Mediterranean: implications for the geological evolution of Avalonia. *Precambrian Research* **290**, 163–83.

Zurbriggen, R. 2015. Ordovician orogeny in the Alps: a reappraisal. *International Journal of Earth Sciences* **104**, 335–50.